Article

Systematic Synthesis, Isolation, and Photophysical Properties of Linear-Shaped Re(I) Oligomers and Polymers with 2#20 Units

Youhei Yamamoto, Shuhei Sawa, Yusuke Funada, Tatsuki Morimoto, Magnus Falkenstro#m, Hiroshi Miyasaka, Sayaka Shishido, Tomoji Ozeki, Kazuhide Koike, and Osamu Ishitani

J. Am. Chem. Soc., **2008**, 130 (44), 14659-14674 • DOI: 10.1021/ja8044579 • Publication Date (Web): 11 October 2008

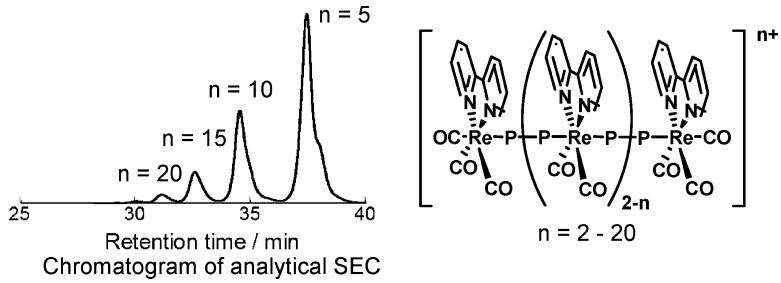

More About This Article

Additional resources and features associated with this article are available within the HTML version:

- Supporting Information
- Access to high resolution figures
- Links to articles and content related to this article
- Copyright permission to reproduce figures and/or text from this article

View the Full Text HTML

J|A|C|S
ARTICLES

Published on Web 10/11/2008

Systematic Synthesis, Isolation, and Photophysical Properties of Linear-Shaped Re(I) Oligomers and Polymers with 2−20 Units

Youhei Yamamoto,[†,‡] Shuhei Sawa,[†] Yusuke Funada,[†] Tatsuki Morimoto,[†] Magnus Falkenström,[§] Hiroshi Miyasaka,[§] Sayaka Shishido,[||] Tomoji Ozeki,[||] Kazuhide Koike,[⊥] and Osamu Ishitani*[,†,‡]

Department of Chemistry and Department of Chemistry and Materials Science, Graduate School of Science and Engineering, Tokyo Institute of Technology, 2-12-1-E1-9 O-okayama, Meguro-ku, Tokyo 152-8551, Japan, SORST, Japan Science and Technology Agency (JST), Japan, Division of Frontier Materials Science, Graduate School of Engineering Science, and Center for Quantum Science and Technology under Extreme Conditions, Osaka University, Toyonaka, Osaka 560-8531, Japan, and National Institute of Advanced Industrial Science and Technology, 16-1 Onogawa, Tsukuba, Ibaraki 305-8569, Japan

Received June 12, 2008; E-mail: ishitani@chem.titech.ac.jp

Abstract: Systematic synthesis routes have been developed for the linear-shaped rhenium(I) oligomers and polymers bridged with bidentate phosphorus ligands, $[Re(N^N)(CO)_3\text{-}PP\text{-}\{Re(N^N)(CO)_2\text{-}PP\text{-}\}_n\text{-}Re(N^N)(CO)_3](PF_6)_{n+2}$ (N^N = diimine, PP = bidentate phosphine, $n = 0-18$). These were isolated by size exclusion chromatography (SEC) and identified by ^{1}H NMR, IR, electrospray ionization Fourier transform mass spectrometry, analytical SEC, and elemental analysis. Crystal structures of $[Re(bpy)(CO)_3\text{-}Ph_2PC{\equiv}CPPh_2\text{-}Re(bpy)(CO)_3](PF_6)_2$, $[Re(bpy)(CO)_3\text{-}Ph_2PC{\equiv}CPPh_2\text{-}Re(bpy)(CO)_2\text{-}Ph_2PC{\equiv}CPPh_2\text{-}Re(bpy)(CO)_3](PF_6)_3$ and $[Re(bpy)(CO)_3\text{-}Ph_2PC_2H_4PPh_2\text{-}\{Re(bpy)(CO)_2Ph_2PC_2H_4PPh_2\text{-}\}_nRe(bpy)(CO)_3](PF_6)_{n+2}$ (bpy = 2,2′-bipyridine, $n = 1, 2$) were obtained, showing that they have interligand $\pi-\pi$ interaction between the bpy ligand and the phenyl groups on the phosphorus ligand. All of the oligomers and polymers synthesized were emissive at room temperature in solution. For the dimers, broad emission was observed with a maximum at 523−545 nm, from the ^{3}MLCT excited-state of the tricarbonyl complex unit, $[Re(N^N)(CO)_3\text{-}PP\text{-}]$. Emission from the longer oligomers and polymers with ≥3 Re(I) units was observed at wavelengths 50−60 nm longer than those of the corresponding dimers. This fact and the emission decay results clearly show that energy transfer from the edge unit to the interior unit occurs with a rate constant of $(0.9 \times 10^8)-(2.5 \times 10^8)$ s^{-1}. The efficient energy transfer and the smaller exclusive volume of the longer Re(I) polymers indicated intermolecular aggregation for these polymers in an MeCN solution.

Introduction

Rod-like polymers constructed of photofunction transition metal complexes, having the ability to show photoinduced energy and electron transfer, are of great interest because of their potential for application in light-harvesting and light-emitting devices and molecular-scale photonic wires.[1] Such transition metal complex polymers fall into three categories: (1) organic main polymer chain derived by addition of metal complexes as pendant groups, such as polystyrene connected with Ru(II) and Os(II) polypyridyl complexes;[2,3] (2) π-conjugated heteroaromatic polymers with diimine parts in a main chain which coordinate to Ru(II) and/or Os(II) polypyridyl complexes, such as poly (2,2′-bipyridine-5,5′-diyl) coordinated to $[Ru(bpy)_2]^{2+}$;[4−6] and (3) metal ions incorporated into the main chain of a polymer.[7−10] Diverse examples of the metal complex polymers in categories (1) and (2) have been synthe-

[†] Department of Chemistry, Graduate School of Science and Engineering, Tokyo Institute of Technology.
[‡] SORST/JST.
[§] Division of Frontier Materials Science, Graduate School of Engineering Science and Center for Quantum Science and Technology under Extreme Conditions, Osaka University.
[||] Department of Chemistry and Materials Science, Graduate School of Science and Engineering, Tokyo Institute of Technology.
[⊥] National Institute of Advanced Industrial Science and Technology.

(1) For reviews, see: (a) BalzaniV.; Moggi, L.; Scandola, F. In *Supramolecular Photochemistry*; Balzani, V., Ed.; D. Reidel: Dordrecht, 1987; pp 1−28. (b) Lehn, J.-M. *Supramolecular Chemistry - Concepts and Perspectives*; VCH: Weinheim, 1995. (c) Sauvage, J. P.; Collin, J. P.; Chambron, J. C.; Guillerez, S.; Coudret, C.; Balzani, V.; Barigelletti, F.; De Cola, L.; Flamigni, L. *Chem. Rev.* **1994**, *94*, 993–1019. (d) Huynh, M. H. V.; Meyer, T. J. *Chem. Rev.* **2007**, *107*, 5004–5064.
(2) (a) Friesen, D. A.; Kajita, T.; Danielson, E.; Meyer, T. J. *Inorg. Chem.* **1998**, *37*, 2756–2762. (b) Dupray, L. M.; Devenney, M.; Striplin, D. R.; Meyer, T. J. *J. Am. Chem. Soc.* **1997**, *119*, 10243–10244. (c) Jones, W. E.; Baxter, S. M.; Strouse, G. F.; Meyer, T. J. *J. Am. Chem. Soc.* **1993**, *115*, 1363–7373.
(3) Serin, J.; Schultze, X.; Adronov, A.; Frechet, J. M. J. *Macromolecules* **2002**, *35*, 5396–5404.
(4) (a) Harriman, A.; Khatry, A.; Ziessel, R. *Res. Chem. Intermed.* **2007**, *33*, 49–62. (b) Harriman, A.; Rostron, S. A.; Khatyr, A.; Ziessel, R. *Faraday Discuss.* **2006**, *131*, 377–391. (c) Harriman, A.; Ziessel, R. *Coord. Chem. Rev.* **1998**, *171*, 331–339. (d) Goeb, S.; DeNicola, A.; Ziessel, R. *J. Organomet. Chem.* **2005**, *70*, 6802–6808.
(5) Connors, P. J.; Tzalis, D.; Dunnick, A. L.; Tor, Y. *Inorg. Chem.* **1998**, *37*, 1121–1123.

sized, and their photophysical properties have been studied in depth. In category (3), however, only two series of transition metal oligomers which can emit in solution at ambient temperature have been reported, even though they should have unique properties because of the contribution of the d orbitals in the transition metal ions to the main polymer chain. One series comprises Pt(II) and Au(I) alkynyl polymers, such as *trans*-$[M(PR_3)_2(-C{\equiv}C\text{-}R\text{-}C{\equiv}C-)_2]_n$ (M = Au or Pt, R = none or aromatic spacer), which emit from a metal-perturbed singlet and triplet intraligand $\pi-\pi^*$ excited states.[11−13] The other series comprises triads constructed with one Os(II) bis-terpyridine and two Ru(II) complexes, where two 2,2′:6′,2″-terpyridine ligands are connected to each other at the 4′ position with a spacer such as *p*-phenylene.[14] Although they emit from the Os(II) unit, the lifetime of the triplet excited state is much shorter than that of the corresponding tris-bipyridine type complex due to a less octahedral geometry of the surrounding ligands. Bis-terpyridine connected with alkyne is a possible bridge ligand, since the corresponding Ru(II) and Os(II) complexes can emit strongly even in solution. However, most reported Ru(II) and Os(II) complexes with such bridge ligands have been diad;[15] no longer oligomer has yet been reported.

The rhenium(I) diimine complexes, *fac*-$[Re(N\text{^}N)(CO)_3(X)]^{n+}$ (N^N = diimine, X = monodentate ligand), have been studied for their unique photochemical properties, such as long lifetime, high emission quantum yield,[16−19] and photocatalysis for CO_2 reduction.[20−22] The Re(I) diimine complexes have also been used as an "L-shaped" building block for supramolecules such as molecular triangles and squares,[23,24] because various diimines and ligands, which are located in the cis position to each other, may be introduced. Unfortunately, the photochemical and thermal stabilities of the three carbonyl ligands on the Re(I) diimine complexes seriously limit the synthesis of "linear" multinuclear Re(I) complexes in which the bridge ligands are coordinated in the trans positions of the central Re(I). Only two linear-shaped trinuclear Re(I) complexes $[\{Re(bpy)(CO)_3(en)\}_2Re(bpy)(CO)_2]^{3+}$ (bpy = 2,2′-bipyridine; en = *trans*-1,2-bis(diphenylphosphino)ethylene) had been reported[25] prior to our preliminary communication.[26a] We have found a novel photochemical ligand substitution reaction of *fac*-$[Re(LL)(CO)_3(PR_3)]^+$, as shown in eq 1.[27] Since only the CO ligand in the position trans to the phosphorus ligand is substituted in this type of photochemical reaction, this discovery provides a new synthesis method for a series of trans-substituted Re(I) mononuclear complexes, namely *cis,trans*-$[Re(LL)(CO)_2(PR_3)(Y)]^+$.[27a] Photochemical ligand substitution can be also applied to a Re(I) dimer connected with a bridge ligand such as 1,2-bis(diphenylphosphino)ethane (et) (eq 2),[26] and we have briefly reported the synthesis of linear trinuclear and tetranuclear Re(I) complexes in a previous communication.[26a]

Below, we report general and systematic synthesis methods for linear-shaped Re(I) oligomers and polymers (Chart 1). We have successfully isolated polymers with up to 20 Re(I) units and identified their precise structures by analytical methods such as electrospray ionization Fourier transform mass spectrometry (ESI FTMS), and size exclusion chromatography (SEC). They can be dissolved in various organic solutions and emit strongly at room temperature in solution. Details of their photophysical properties are reported.

Results and Discussion

We used the synthetic strategy "*complex as metal*" and "*complex as ligand*" proposed by Balzani[28] for the synthesis of linear-shaped oligo- and polynuclear Re(I) complexes. We

(6) (a) Hayasida, N.; Yamamoto, T. *Bull. Chem. Soc. Jpn.* **1999**, *72*, 1153–1162. (b) Yamamoto, T.; Maruyama, T.; Zhou, Z.-H.; Ito, T.; Fukuda, T.; Yoneda, Y.; Begum, F.; Ikeda, T.; Sasaki, S.; Takezoe, H.; Fukuda, A.; Kubotall, K. *J. Am. Chem. Soc.* **1994**, *116*, 4832–4845.
(7) Hissler, M.; El-ghayoury, A.; Harriman, A.; Ziessel, R. *Angew. Chem., Int. Ed.* **1998**, *37*, 1717–1720.
(8) (a) Knapp, R.; Kelch, S.; Schmelz, O.; Rehahn, M. *Macromol. Symp.* **2003**, *204*, 267–286. (b) Kelch, S.; Rehahn, M. *Chem. Commun.* **1999**, 1123–1124. (c) Kelch, S.; Rehahn, M. *Macromolecules* **1999**, *32*, 5818–5828.
(9) Cho, T. J.; Moorefield, C. N.; Hwang, S.-H.; Wang, P.; Godínez, L. A.; Bustos, E.; Newkome, G. R. *Eur. J. Org. Chem.* **2006**, 4193–4200.
(10) Hayashida, N.; Yamamoto, T. *Bull. Chem. Soc. Jpn.* **1999**, *72*, 1153–1162.
(11) (a) Yam, V. W. W.; Wong, K. M. C. In *Molecular Wires*; De Cola, L., Ed.; Springer: Berlin, 2005; Vol. 257, pp 1−32. (b) Yam, V. W. W.; Cheng, E. C. C.; In *Photochemistry and Photophysics of Coordination Compounds II*; Balzani, V., Campagna, S., Eds.; Springer: Berlin, 2007; Vol. 281, pp 269−310. (c) Yam, V. W. W.; Lo, K. K. W.; Wong, K. M. C. *J. Organomet. Chem.* **1999**, *578*, 3–30.
(12) Vicente, J.; Chicote, M. T.; Alvarez-Falcon, M. M.; Fox, M. A.; Bautista, D. *Organometallics* **2003**, *22*, 4792–4797.
(13) (a) Yamamoto, Y.; Shiotsuka, M.; Onaka, S. *J. Organomet. Chem.* **2004**, *689*, 2905–2911. (b) Shiotsuka, M.; Yamamoto, Y.; Okuno, S.; Kitou, M.; Nozaki, K.; Onaka, S. *Chem. Commun.* **2002**, 590–591.
(14) (a) Harriman, A.; Ziessel, R. *Coord. Chem. Rev.* **1998**, *171*, 331–339. (b) Barigelletti, F.; Flamigni, L.; Balzani, V.; Collin, J.-P.; Sauvage, J.-P.; Sour, A.; Constable, E. C.; Thompson, A. M. W. C. *J. Am. Chem. Soc.* **1994**, *116*, 7692–7699. (c) Benniston, A. C.; Harriman, A.; Li, P.; Patel, P. V.; Sams, C. A. *Chem. Eur. J.* **2008**, *14*, 1710–1717.
(15) (a) Harriman, A.; Hissler, M.; Khatyr, A; Ziessel, R. *Eur. J. Inorg. Chem.* **2003**, 955–959. (b) Grosshenny, V.; Harriman, A.; Ziessel, R. *Angew. Chem., Int. Ed. Engl.* **1995**, *34*, 1100–1102.
(16) Luong, J. C.; Nadjo, L.; Wrighton, M. S. *J. Am. Chem. Soc.* **1978**, *100*, 5790–5795.
(17) (a) Worl, L. A.; Strouse, F. S.; Younathan, J. N.; Baxter, S. M.; Meyer, T. J. *J. Am. Chem. Soc.* **1990**, *112*, 7571–7578. (b) Caspar, J. V.; Meyer, T. J. *J. Phys. Chem.* **1983**, *87*, 952–957. (c) Caspar, J. V.; Meyer, T. J. *J. Phys. Chem.* **1983**, *87*, 952–957.
(18) Schutte, E.; Helms, J. B.; Woessner, S. M.; Bowen, J.; Sullivan, B. P. *Inorg. Chem.* **1998**, *37*, 2618–2619.
(19) Hori, H.; Koike, K.; Ishizuka, M.; Takeuchi, K.; Ibusuki, T.; Ishitani, O. *J. Organomet. Chem.* **1997**, *530*, 169–176.
(20) Hawecker, J.; Lehn, J.-M.; Ziessel, R. *Helv. Chim. Acta* **1986**, *69*, 1990–2012.
(21) Kurz, P.; Probst, B.; Spingler, B.; Alberto, R. *Eur. J. Inorg. Chem.* **2006**, *15*, 2966–2974.
(22) (a) Takeda, H.; Koike, K.; Inoue, H.; Ishitani, O. *J. Am. Chem. Soc.* **2008**, *130*, 2023–2031. (b) Koike, K.; Hori, H.; Ishizuka, M.; Westwell, J. R.; Takeuchi, K.; Ibusuki, T.; Enjouji, K.; Konno, H.; Sakamoto, K.; Ishitani, O. *Organometallics* **1997**, *16*, 5724–5729. (c) Hori, H.; Ishihara, J.; Koike, K.; Takeuchi, K.; Ibusuki, T.; Ishitani, O. *J. Photochem. Photobiol., A* **1999**, *120*, 119–124.
(23) (a) O'Donnell, J. L.; Zuo, X.; Goshe, A. J.; Sarkisov, L.; Snurr, R. Q.; Hupp, J. T.; Tiede, D. M. *J. Am. Chem. Soc.* **2007**, *129*, 1578–1585. (b) Hupp, J. T. In *Structure Bonding (Berlin)*; Alessio, E., Ed.; Springer: Berlin, 2006; Vol. 121, pp 145−165.
(24) Barbazán, P.; Carballo, R.; Casas, J. S.; Garcia-Martinez, E.; Pereiras-Gabián, G.; Sánchez, A.; Vazquez-López, E. M. *Inorg. Chem.* **2006**, *45*, 7323–7330.
(25) Woessner, S. M.; Helms, J. B.; Lantzky, K. M.; Sullivan, B. P. *Inorg. Chem.* **1999**, *38*, 4378–4379.
(26) (a) Ishitani, O.; Kanai, K.; Yamada, Y.; Sakamoto, K. *Chem. Commun.* **2001**, 1514–1515. (b) DelNegro, A. S.; Woessner, S. M.; Sullivan, B. P.; Dattelbaum, D. M.; Schoonover, J. R. *Inorg. Chem.* **2001**, *40*, 5056–5057.
(27) (a) Koike, K.; Tanabe, J.; Toyama, S.; Tsubaki, H.; Sakamoto, K.; Westwell, J. R.; Johnson, F. P. A.; Hori, H.; Saitoh, H.; Ishitani, O. *Inorg. Chem.* **2000**, *39*, 2777–2783. (b) Koike, K.; Okoshi, N.; Hori, H.; Takeuchi, K.; Ishitani, O.; Tsubaki, H.; Clark, I. P.; George, M. W.; Johnson, F. P. A.; Turner, J. J. *J. Am. Chem. Soc.* **2002**, *124*, 11448–11455.
(28) Balzani, V.; Juris, A.; Venturi, M.; Campagna, S.; Serroni, S. *Chem. Rev.* **1996**, *96*, 759–834.

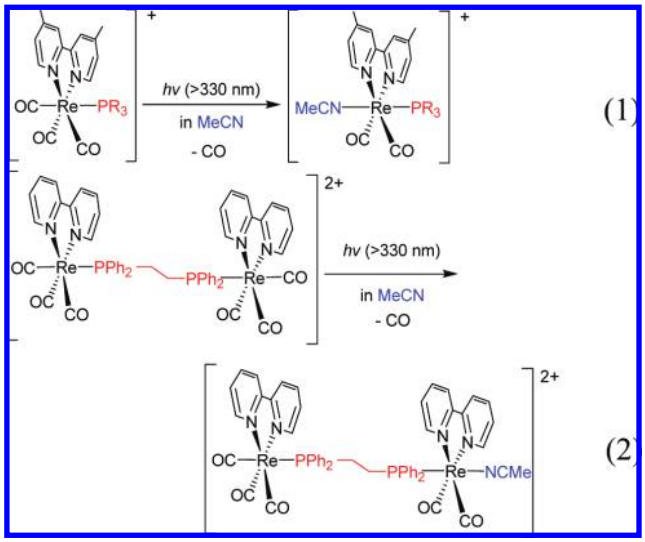

prepared "*complexes as metal*", where an easily replaceable $CF_3SO_3^-$ anion or a solvent molecule coordinates in the trans position to a phosphorus bridge ligand, employing a photochemical ligand substitution reaction of Re(I) monomers or oligomers as described below. We prepared "*complex as ligand*" having one or two η^1-type bidentatable phosphorus ligand(s), of which one side coordinates to the central metal and the other side is available for coordination to a further metal (Chart 1). Coupling reactions or polymerization of these complexes gave a series of linear-shaped oligo- and polynuclear Re(I) diimine complexes. The relatively high solubility of these complexes in polar organic solvents such as MeCN and MeOH allowed isolation of polymers with up to 20 Re(I) units, using SEC.

As representative examples, synthesis of the linear-shaped oligo- and polynuclear Re(I) complexes consisting of bis(diphenylphosphino)acetylene (ac) as a bidentatable phosphorus ligand and 2,2′-bipyridine (bpy) are described. The abbreviation $[\mathbf{Re}N\mathbf{ac}]^{N+}$ is used for complexes with two $Re(bpy)(CO)_3$ units in both edges (*N* denotes the number of Re(I) units; **ac** indicates that ac is the bridge ligand). "*Complex as metal*" and "*complex as ligand*", in which one or two CO ligand(s) in the edge unit(s) are substituted with L′ ($m = 1$, L′ = $CF_3SO_3^-$; $m = 0$, L′ = CH_2Cl_2 or MeCN) or **ac**, are respectively abbreviated as $[\mathbf{Re}N\mathbf{ac}(\mathbf{L'})_1]^{(N-m)+}$ or $[\mathbf{Re}N\mathbf{ac}(\mathbf{L'})_2]^{(N-2m)+}$ (*complexes as metal*), and $[\mathbf{Re}N\mathbf{ac}(\boldsymbol{\eta}^1\mathbf{\text{-}ac})_{1\text{ or }2}]^{N+}$ (*complex as ligand*) (Chart 1).

Synthesis of Di-, Tri-, and Tetranuclear Re(I) Complexes. The dinuclear complex $[Re(bpy)(CO)_3(ac)Re(bpy)(CO)_3]^{2+}$ ($[\mathbf{Re2ac}]^{2+}$) was obtained in high yield by thermal reaction of *fac*-$Re(bpy)(CO)_3(CF_3SO_3)$ with a 0.5 equiv of ac. It was then used as a precursor for the synthesis of oligomers and polymers. Scheme 1 summarizes the synthesis of the trinuclear complex $[Re(bpy)(CO)_3(ac)Re(bpy)(CO)_2(ac)Re(bpy)(CO)_3]^{3+}$ ($[\mathbf{Re3ac}]^{3+}$) and the tetranuclear complex $[Re(bpy)(CO)_3(ac)\text{-}\{Re(bpy)(CO)_2(ac)\}_2Re(bpy)(CO)_3]^{4+}$ ($[\mathbf{Re4ac}]^{4+}$). A dichloromethane solution containing $CF_3SO_3^-$ salts of $[\mathbf{Re2ac}]^{2+}$ was irradiated under an Ar atmosphere for 30 min, giving $[Re(bpy)(CO)_3(ac)Re(bpy)(CO)_2(CF_3SO_3)]^+$ ($[\mathbf{Re2ac}(\mathbf{CF_3SO_3})_1]^+$) where one carbonyl ligand in the position trans to the ac ligand was substituted with $CF_3SO_3^-$. Thermal reaction of $[\mathbf{Re2ac}(\mathbf{CF_3SO_3})_1]^+$ with excess ac in CH_2Cl_2 led to substitution of the $CF_3SO_3^-$ ligand by ac, to give $[Re(bpy)(CO)_3\text{-}(ac)Re(bpy)(CO)_2(\eta^1\text{-}ac)]^{2+}$ ($[\mathbf{Re2ac}(\boldsymbol{\eta}^1\mathbf{\text{-}ac})_1]^{2+}$), where ac in the edge ($\boldsymbol{\eta}^1$**-ac**) works as a monodentate ligand and can coordinate with another metal center. A coupling reaction of $[\mathbf{Re2ac}(\boldsymbol{\eta}^1\mathbf{\text{-}ac})_1]^{2+}$ with *fac*-$Re(bpy)(CO)_3(CF_3SO_3)$ gives $[\mathbf{Re3ac}]^{3+}$ in a 82% isolated yield. For preparation of $[\mathbf{Re4ac}]^{4+}$, $[\mathbf{Re2ac}(\mathbf{CF_3SO_3})_1]^+$ reacted with ac in a 2:1 molar ratio; the isolated yield was 72%. Good yields were also obtained in the synthesis of other tri- and tetranuclear complexes with various bidentate phosphorus and diimine ligands, as summarized in Table 1.

Chart 1. Structures and Abbreviations of Synthesized Oligo- and Polynuclear Complexes, "*Complex as Metal*", "*Complex as Ligand*", Diimine Ligands LL, and Bidentate Phosphorus Ligands **X** (PPh_2-R-PPh_2)

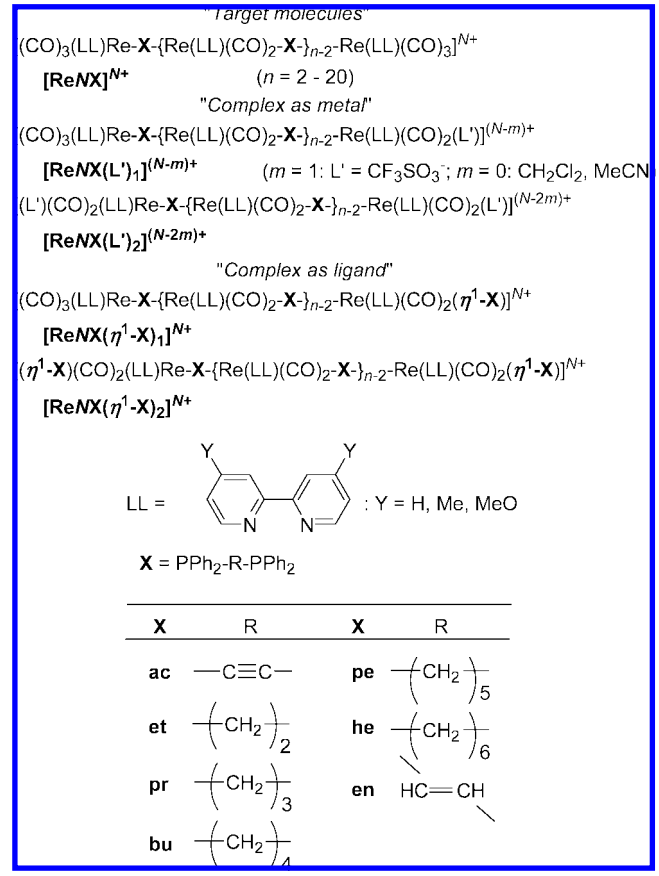

Photochemical Ligand Substitution Reactions of Re(I) Oligomers. As described above, brief irradiation of a CH_2Cl_2 solution containing $[\mathbf{Re2ac}]^{2+}(CF_3SO_3^-)_2$ selectively yields the unsymmetrical dimer $[\mathbf{Re2ac}(\mathbf{CF_3SO_3})_1]^+$. Although $[\mathbf{Re2ac}(\mathbf{CF_3SO_3})_1]^+$ was relatively stable against irradiation, because of efficient energy transfer from the tricarbonyl Re(I) unit to another biscarbonyl Re(I) unit (eq 3), longer irradiation times (such as for 15 h) caused further substitution of the CO ligand(s) to give two products, $[\{Re(bpy)(CO)_2(CF_3SO_3)\}_2(ac)]$ ($[\mathbf{Re2ac}(\mathbf{CF_3SO_3})_2]$) and $[Re(bpy)(CO)_2(CF_3SO_3)(ac)Re(bpy)\text{-}(CO)(CF_3SO_3)(L')]$ (L′ should be CH_2Cl_2 as solvent), where $[\mathbf{Re2ac}(\mathbf{CF_3SO_3})_1]^+$ still remained in the solution (Figure S1 in Supporting Information).

$$[Re^*(bpy)(CO)_3(ac)Re(bpy)(CO)_2(CF_3SO_3)]^+ \rightarrow [Re(bpy)(CO)_3(ac)Re^*(bpy)(CO)_2(CF_3SO_3)]^+ \quad (3)$$

The photochemical behavior of $[\mathbf{Re3ac}]^{3+}$ and $[\mathbf{Re4ac}]^{4+}$ was different from that of $[\mathbf{Re2ac}]^{2+}$. Even after 45 min irradiation, much $[\mathbf{Re4ac}]^{4+}$ remained in the solution, while the disubstituted product $[\mathbf{Re4ac}(\mathbf{CF_3SO_3})_2]^{2+}$ was produced accompanied by

Scheme 1. Synthesis of Linear-Shaped Tri- and Tetranuclear Rhenium(I) Complexes[a]

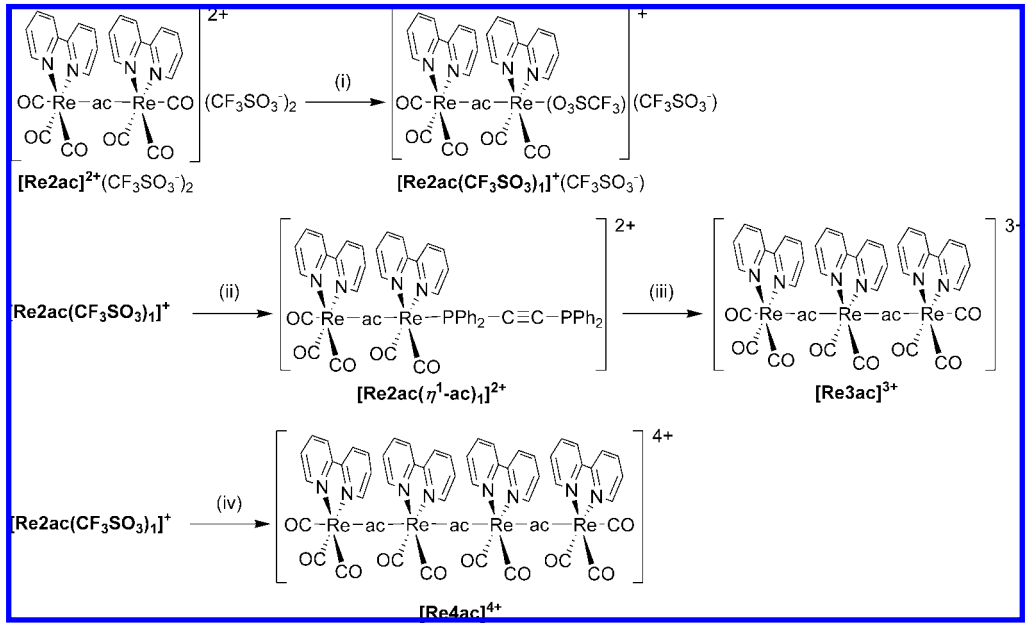

[a] Reagents and reaction conditions: (i) *hν* (>330 nm) in CH_2Cl_2 for 30 min; (ii) excess ac in CH_2Cl_2 at room temperature for 1 day, then at 40 °C for 1 day; (iii) *fac*-Re(bpy)$(CO)_3(CF_3SO_3)$ in CH_2Cl_2 at room temperature for 1 day, then at 40 °C for 1 day; (iv) ac (0.5 equiv) in CH_2Cl_2 at room temperature for 1 day, then at 40 °C for 1 day.

Table 1. Isolated Yields of Linear-Shaped Di-, Tri-, and Tetranuclear Complexes with Various Bidentate Phosphorus Ligands

		yield/%								
	LL =	bpy							dmb[b]	MeObpy[c]
complex[a]	X =	ac	et	pr	bu	pe	he	en	ac	ac
[Re2X]$^{2+}$		94	95	92	93	92	93	94	90	91
[Re3X]$^{3+}$		82	63	70	81	57	59	62	64	41
[Re4X]$^{4+}$		72	75	60	68	60	63	85	75	81

[a] Isolated as PF_6^- salts. [b] 4,4′-Dimethy-2,2′-bipyridine. [c] 4,4′-Dimethoxy-2,2′-bipyridine.

[Re4ac(CF$_3$SO$_3$)$_1$]$^{3+}$ (Figure S2b in Supporting Information). Four tetranuclear complexes, i.e., **[Re4ac]$^{4+}$**, **[Re4ac(CF$_3$SO$_3$)$_1$]$^{3+}$**, **[Re4ac(CF$_3$SO$_3$)$_2$]$^{2+}$**, and **[Re4ac(CF$_3$SO$_3$)$_3$]$^{+}$** coexisted in the solution after 1.5 h irradiation (Figure S2c in Supporting Information). The trimer **[Re3ac]$^{3+}$** had similar photochemical reactivity to **[Re4ac]$^{4+}$**. As described in the "Emission" section, intramolecular energy transfer took place from the excited edge Re(I) unit to the interior Re(I) unit, so that the lifetime of the excited state of the edge unit in both **[Re3ac]$^{3+}$** and **[Re4ac]$^{4+}$** was much shorter (~10 ns) than that of **[Re2ac]$^{2+}$**. We have reported previously that photochemical ligand substitution reaction of mononuclear Re(I) complexes with a phosphorus ligand, *fac*-[Re(bpy)$(CO)_3(PR_3)]^+$, proceeds via the triplet metal-centered excited state (^{3}ML), which is thermally in equilibrium with the emissive and lowest excited state, i.e. a triplet metal-to-ligand charge transfer excited state (^{3}MLCT). Since it is reasonable to suppose that the photochemical ligand substitution reaction of the multinuclear complexes also proceeds via the same mechanism, the shorter excited lifetime of the edge Re(I) unit in trimer and tetramer because of the efficient energy transfer explains why the efficiency of the photochemical ligand substitution of **[Re3ac]$^{3+}$** and **[Re4ac]$^{4+}$** was much lower than that of **[Re2ac]$^{2+}$**.

Synthesis of Complexes with 5−8 Re(I) Units. Complexes with 5−8 Re(I) units were synthesized using $CF_3SO_3^-$ salts of **[Re3ac]$^{3+}$** or **[Re4ac]$^{4+}$** as starting complexes. The synthesis is shown in Scheme 2. A dichloromethane solution containing $CF_3SO_3^-$ salts of **[Re3ac]$^{3+}$** was irradiated for 1 h to give a mixture of **[Re3ac(CF$_3$SO$_3$)$_1$]$^{2+}$** and **[Re3ac(CF$_3$SO$_3$)$_2$]$^{+}$**, where one or two carbonyl ligand(s) in one or both edge unit(s) are substituted with $CF_3SO_3^-$. The mixture also contained the starting complex **[Re3ac]$^{3+}$**, but further irradiation gave a complex with a monocarbonyl rhenium(I) unit in the edge, [Re(bpy)$(CO)_2(CF_3SO_3)$(ac)Re(bpy)$(CO)_2$(ac)Re(bpy)(CO)-$(CF_3SO_3)_2$], as byproduct. The ratio of **[Re3ac(CF$_3$SO$_3$)$_1$]$^{2+}$**, **[Re3ac(CF$_3$SO$_3$)$_2$]$^{+}$**, and **[Re3ac]$^{3+}$** was approximately 3:1:5. A thermal reaction of this mixture with **[Re2ac(η^1-ac)$_1$]$^{2+}$** as "complex as ligand" gave both [Re(bpy)$(CO)_3$(ac){Re(bpy)-$(CO)_2$(ac)}$_3$Re(bpy)$(CO)_3]^{5+}$(**[Re5ac]$^{5+}$**)and[Re(bpy)$(CO)_3$(ac)-{Re(bpy)$(CO)_2$(ac)}$_5$Re(bpy)$(CO)_3]^{7+}$ (**[Re7ac]$^{7+}$**) in 32% and 9% yields, respectively, along with 53% recovery of **[Re3ac]$^{3+}$**. By a similar method, using **[Re4ac]$^{4+}$** instead of **[Re3ac]$^{3+}$** as a precursor complex, hexa- and octanuclear complexes [Re(bpy)$(CO)_3$(ac){Re(bpy)$(CO)_2$(ac)}$_n$Re(bpy)$(CO)_3]^{(n+2)+}$ (n = 4, **[Re6ac]$^{6+}$**; n = 6, **[Re8ac]$^{8+}$**) were synthesized in 23% and 3% yields, respectively, with 43% recovery of **[Re4ac]$^{4+}$**.

The corresponding multinuclear Re(I) complexes with et as bridge ligands were obtained by a similar method. The yields were 37% for [Re(bpy)$(CO)_3$(et){Re(bpy)$(CO)_2$(et)}$_3$-Re(bpy)$(CO)_3]^{5+}$ (**[Re5et]$^{5+}$**) and 5% for [Re(bpy)$(CO)_3$(et)-{Re(bpy)$(CO)_2$(et)}$_5$Re(bpy)$(CO)_3]^{7+}$ (**[Re7et]$^{7+}$**), with 65% recovery of the starting complex **[Re3et]$^{3+}$**. These methods should therefore be applicable to the synthesis of other complexes connected by various bidentate phosphorus ligands.

We have developed another method for selective synthesis of **[Re5ac]$^{5+}$** in higher yield. A thermal reaction of *fac*-Re(bpy)$(CO)_3(CF_3SO_3)$ with excess ac in a THF solution gave *fac*-[Re(bpy)$(CO)_3(\eta^1$-ac)$]^+$. This solution was irradiated for 1 night, giving *cis,trans*-[Re(bpy)$(CO)_2(\eta^1$-ac$)_2]^+$ (eq 4). A thermal reaction of *cis,trans*-[Re(bpy)$(CO)_2(\eta^1$-ac$)_2]^+$ with two equivalents of **[Re2ac(CF$_3$SO$_3$)$_1$]$^{+}$** in CH_2Cl_2 gave **[Re5ac]$^{5+}$** in 66% yield (eq 5). Unfortunately, this method cannot be

Scheme 2. Synthesis of Oligomers with 5 and 7 Re(I) Units[a]

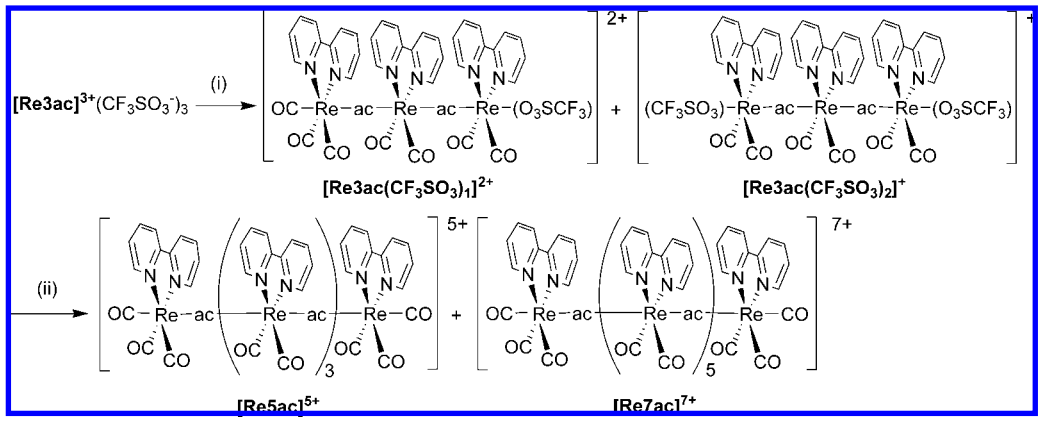

[a] Reagents and reaction conditions: (i) *hv* (>330 nm) in CH_2Cl_2 for 1 h; (ii) $[Re2ac(\eta^1\text{-}ac)_1]^{2+}$ in CH_2Cl_2 at room temperature for 1 day, then at 40 °C for 1 day.

Scheme 3. Synthesis of Linear-Shaped Re(I) Polymers[a]

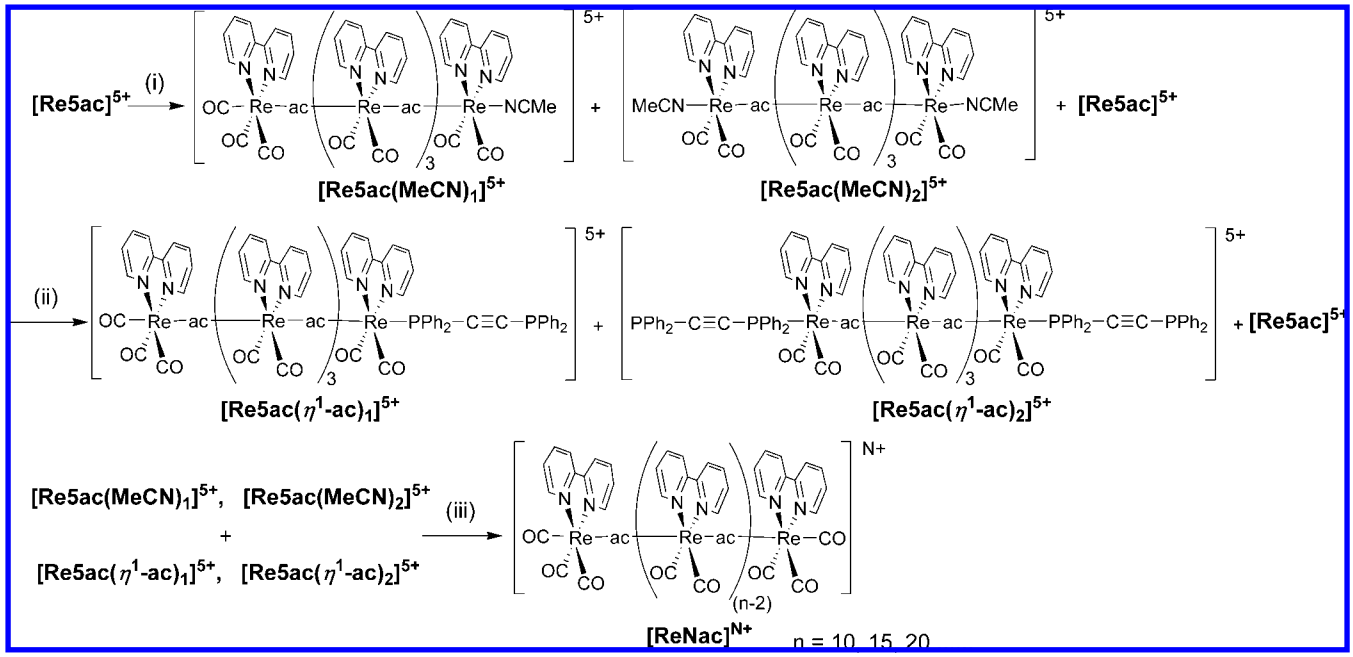

[a] Reagents and reaction conditions: (i) *hv* (>330 nm) in MeCN for 1 h; (ii) excess ac in acetone/THF (1:1) at room temperature for 1 day, then at 40 °C for 1 day; (iii) in acetone/THF (1:1) at room temperature for 1 day, then at 40 °C for 2 days.

applied to synthesize pentanuclear complexes with other bidentate phosphorus ligands, such as et, because irradiation of these complexes gave mainly *cis*-$[Re(bpy)(\eta^2\text{-et})(CO)_2]^+$ even in the presence of excess phosphorus ligand (eq 6).

Polymerization. We attempted the polymerization of Re(I) complexes using **[Re5ac]**$^{5+}$ as a starting complex (Scheme 3), because **[Re5ac]**$^{5+}$ can be synthesized in high yield by relatively simple procedures, as described above. An acetonitrile solution containing the PF_6^- salts of **[Re5ac]**$^{5+}$ was irradiated for 1 h, giving a mixture of $[Re5ac(MeCN)_1]^{5+}$, $[Re5ac(MeCN)_2]^{5+}$, and **[Re5ac]**$^{5+}$. After evaporation of the solvent, one-half of the residue reacted with excess ac in a mixed solution of acetone and THF (1:1 v/v) under an Ar atmosphere, generating a mixture of $[Re5ac(\eta^1\text{-}ac)_1]^{5+}$ and $[Re5ac(\eta^1\text{-}ac)_2]^{5+}$. Both mixtures which were "*complexes as metals*", i.e., $[Re5ac(MeCN)_1]^{5+}$ and $[Re5ac(MeCN)_2]^{5+}$, and "*complexes as ligands*", i.e., $[Re5ac(\eta^1\text{-}ac)_1]^{5+}$ and $[Re5ac(\eta^1\text{-}ac)_2]^{5+}$, were dissolved in an acetone/THF (1:1 v/v) mixed solution, and was a maintained at 40 °C for 2 days. Figure S3 in Supporting Information shows a size exclusion chromatogram of the crude product. This result clearly indicates the formation of various Re(I) polymers in which the number of rhenium(I) units is a multiple of 5, such as **[Re10ac]**$^{10+}$, **[Re15ac]**$^{15+}$, **[Re20ac]**$^{20+}$, and **[Re25ac]**$^{25+}$. Some of the products, **[Re10ac]**$^{10+}$, **[Re15ac]**$^{15+}$, and **[Re20ac]**$^{20+}$, were isolated using SEC as described below, in yields of 16%, 6%, and 4%, respectively, with 50% recovery of **[Re5ac]**$^{5+}$. Polymers with more than 20 Re(I) units could not be isolated, because of their low yields. By a similar method, using **[Re4ac]**$^{4+}$ instead of **[Re5ac]**$^{5+}$ as a precursor complex, **[Re8ac]**$^{8+}$, **[Re12ac]**$^{12+}$, and **[Re16ac]**$^{16+}$ were obtained in yields of 19%, 14%, and 3%,respectively, with 55% recovery of **[Re4ac]**$^{4+}$.

Isolation and Identification. We isolated the Re(I) oligomers and polymers by SEC, using a hydrophilic column for gel filtration and a methanol/acetonitrile (1:1) mixed eluent contain-

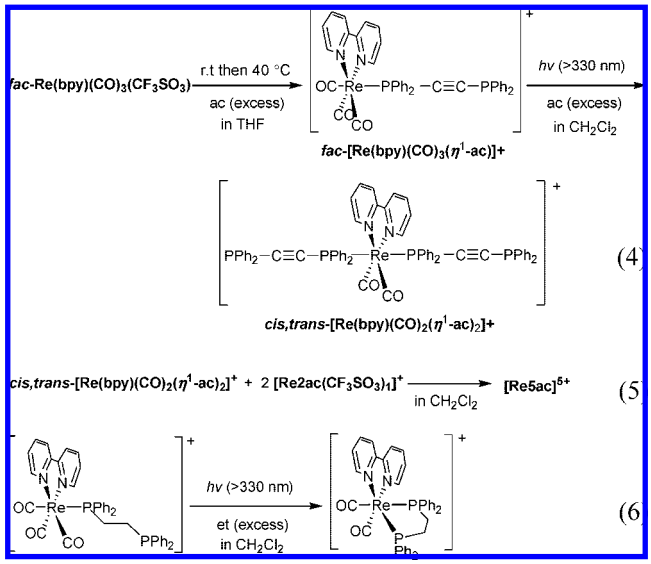

ing $CH_3CO_2NH_4$ (0.15 M).[29] This method was useful for isolation because of the relatively high solubilities of the complexes in polar solvents, and the large difference in molecular weights of the polymers in the crude products. Chromatograms of analytical SEC for the crude products and the isolated **[Re5ac]**$^{5+}$, **[Re10ac]**$^{10+}$, **[Re15ac]**$^{15+}$, and **[Re20ac]**$^{20+}$ are shown in Figure S3 in Supporting Information. The other Re(I) oligomers and polymers could also be isolated from the reaction mixture by a similar method using SEC.

The isolated Re(I) oligomers and polymers were identified by a combination of ^{1}H NMR, IR, electrospray ionization Fourier transform mass spectrometry (ESI FTMS), analytical SEC, and elemental analysis. High-resolution ESI FTMS is a particularly powerful technique for identifying oligomers. As an example, the mass spectrum of **[Re8ac]**$^{8+}(PF_6^-)_8$ is shown in Figure 1. There are five peaks, each attributable to **[Re8ac]**$^{8+}$ with a different number of PF_6^-, i.e., $[\mathbf{M} + n(PF_6^-)]^{(8-n)+}$ ($n = 0-4$); virtually no fragmentation peaks were observed. Figure 2a shows a scale-extended spectrum of the peaks attributed to $[\mathbf{M} + PF_6^-]^{7+}$. This identification is supported by the strong similarities with the calculated spectrum shown in Figure 2b, as follows: (1) the *m*/*z* values are in good agreement with the calculated values with mass accuracy of <3.5 ppm; (2) The separations of the individual isotope peaks are 0.1431 ± 0.0001 amu, which is reliable evidence that the peaks are due to a cation with 7+ charges; (3) the patterns for the isotope distribution in the observed and calculated peaks are almost identical. The other peaks observed were also in good agreement with the calculated values. Similar results are obtained for **[Re2ac]**$^{2+}$ - **[Re7ac]**$^{7+}$. Although fragmentation peaks corresponding one CO-ligand were replaced by one eluent molecule (MeCN) were detected in the case of polymers with 10−16 Re(I) units, the main parent ion peaks were also observed and agree well with the calculated values. No parent peak was detected for polymers with >16 Re(I) units.

Figure 3 shows aromatic proton peaks in ^{1}H NMR spectra of **[Re2ac]**$^{2+}$, **[Re3ac]**$^{3+}$, **[Re6ac]**$^{6+}$, **[Re8ac]**$^{8+}$, and **[Re20ac]**$^{20+}$ measured in acetone-d_3 at room temperature. Signals attributed to the protons in the bpy ligand can be divided into three groups: (i) edge units having structure [Re(bpy)(CO)$_3$]-; (ii) the next units from the edge -[Re(bpy)(CO)$_2$]-, located between [Re(bpy)(CO)$_3$]- and -[Re(bpy)(CO)$_2$]-; (iii) deeper interior units -[Re(bpy)(CO)$_2$]- which are between two -[Re(bpy)(CO)$_2$]- units. The proton signals attributed to the group (i) were observed at lower magnetic fields than the other groups, because of the three CO ligands which have greater π-acidity than the phosphorus ligands, and probably because there are only two phenyl groups on the phosphorus ligand close to the bpy ligand, but four phenyl groups for groups (ii) and (iii). Proton peaks attributed to the group (iii) were not observed for **[Re3ac]**$^{3+}$. The integrated areas for the protons in the group (iii) increased for longer Re polymers: the area ratios for groups (i), (ii), and (iii) were about 2:2:1, 2:2:2, 2:2:3, and 2:2:4 for **[Re5ac]**$^{5+}$ to **[Re8ac]**$^{8+}$, respectively. The relationship between the number of Re(I) units and the ratios of the integrated areas $A(H_5^i + H_5^{ii})/A(H_6^{iii})$ ($n = 3, 4, 6$) is shown with black circles in Figure 4 for **[Re2ac]**$^{2+}$ to **[Re16ac]**$^{16+}$ for which structures were conclusively determined by ESI FTMS, as described above. The good linear relationship demonstrates that this figure is useful for determining the number of Re(I) units in those polymers for which parent ion peaks could not be observed by ESI FTMS. The calibration line indicates that the longest isolated polymer made from **[Re5ac]**$^{5+}$ as a starting complex has 20.4 ± 2.0 Re(I) units (the red circle in Figure 4).

FT IR spectra of the oligomers and polymers provide further information about the number of Re(I) units. Figure 5shows IR spectra of **[Re2ac]**$^{2+}$ to **[Re8ac]**$^{8+}$ in the ν(CO) region measured in MeCN at room temperature. IR spectra reported for mono-

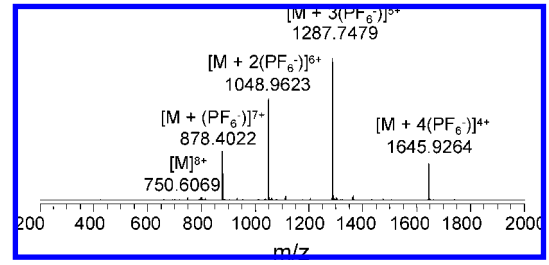

Figure 1. ESI FTMS spectrum of **[Re8ac]**$^{8+}(PF_6^-)_8$. The eluent was MeCN.

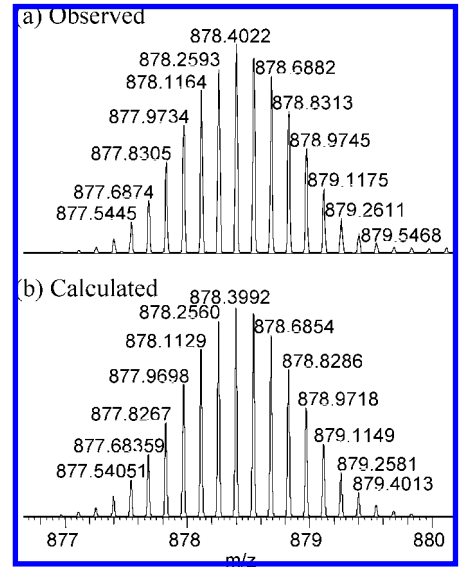

Figure 2. ESI FTMS spectrum of the scale-extended segment for the seven charged $[\mathbf{M} + (PF_6^-)]^{7+}$ (a) and calculated isotope distribution patterns (b).

(29) Takeda, H.; Yamamoto, Y.; Nishiura, C.; Ishitani, O. *Anal. Sci.* **2006**, *22*, 545–549.

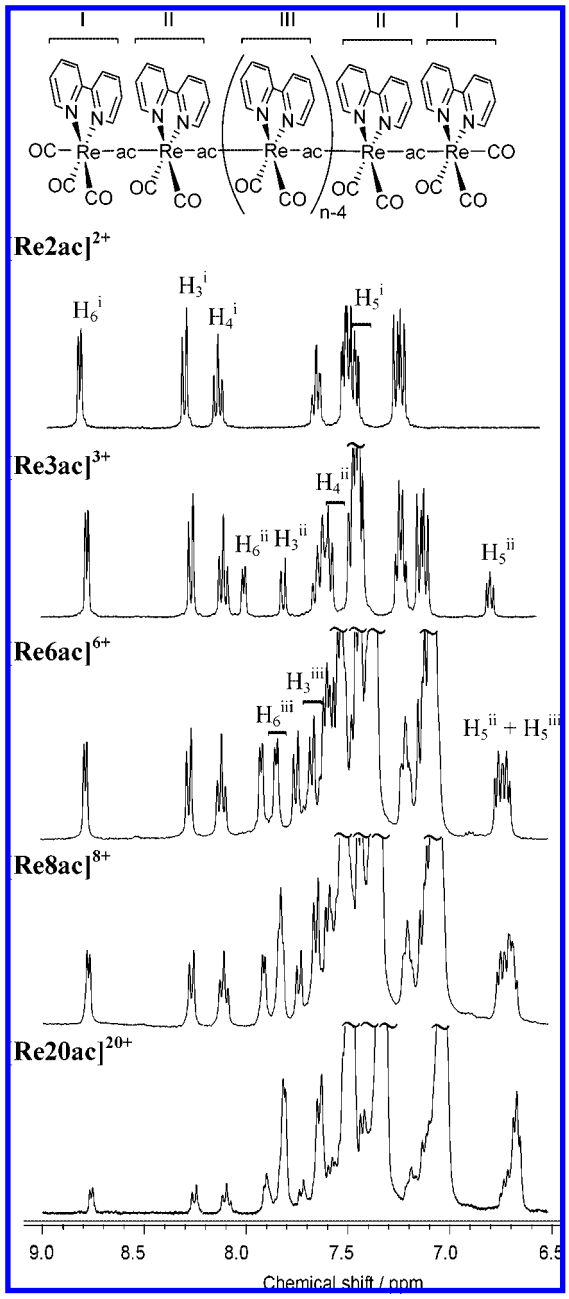

Figure 3. Aromatic regions in ^{1}H NMR spectra of **[Re2ac]$^{2+}$**, **[Re3ac]$^{3+}$**, **[Re6ac]$^{6+}$**, **[Re8ac]$^{8+}$**, and **[Re20ac]$^{20+}$** measured in acetone-d_3 at room temperature.

nuclear *fac*-[Re(LL)(CO)$_3$(PR$_3$)]$^+$ and *cis,trans*-[Re(LL)(CO)$_2$(PR$_3$)(PR′$_3$)]$^+$ type complexes clearly indicate that these complexes have three and two ν(CO) peaks, with similar absorbance, respectively.[19,27,30] The ratios of the areas between the peaks at 1885 cm^{-1} and 2048 cm^{-1}, attributable to the edge and interior units respectively, are plotted against the number of Re(I) units in Figure 6. The number of Re(I) units in the longest isolated polymer can also be calculated, as 20.1 ± 0.4 units for the polymers made from **[Re5ac]$^{5+}$** based on this figure. This result is consistent with those obtained by ^{1}H NMR measurement as described above.

Analytical SEC can also be used to determine the molecular weights of the Re(I) polymers.[29] Figure 7 shows the plots of

(30) Smithback, J. L.; Helms, J. B.; Schutte, E.; Woessner, S. M.; Sullivan, B. P. *Inorg. Chem.* **2006**, *45*, 2163–2174.

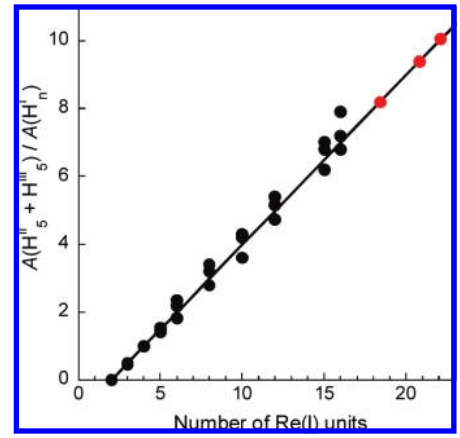

Figure 4. Relationship between the number of Re(I) units in the oligomers and polymers and ratios of the integrated areas of their ^{1}H NMR signals, $A(H^{i}_{5} + H^{ii}_{5})/A(H^{iii}_{6})$ (n = 3, 4, 6), measured in acetone-d_3 at room temperature. See the structure as shown in Figure 3 for numbering of the protons. The red circle is the longest isolated polymer made from **[Re5ac]$^{5+}$**.

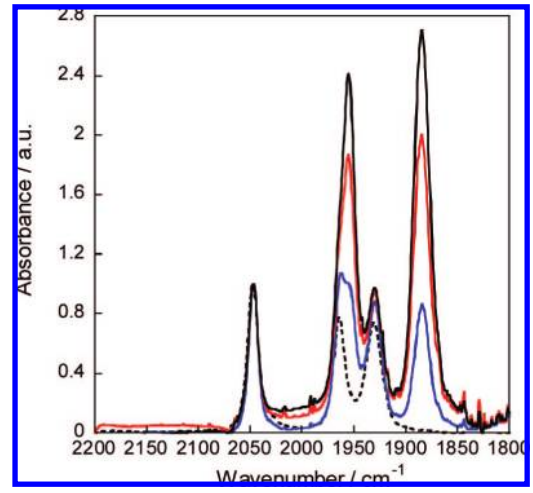

Figure 5. IR spectra of **[Re2ac]$^{2+}$** (dotted line), **[Re4ac]$^{4+}$** (blue line), **[Re6ac]$^{6+}$** (red line), and **[Re8ac]$^{8+}$** (solid black line) measured in MeCN. They are standardized by the absorbance at 2048 cm^{-1}.

the logarithms of the molecular weights (excluding those of counter anions) against the distribution coefficient K_{SEC}. A straight line can be drawn for the polymers with 6−16 Re(I) units (eq 7), as shown in Figure 7, but the data for the shorter oligomers could not be fitted by this line. This demonstrates that the distribution coefficients (K_{SEC}) for longer Re(I) polymers (**[Re6ac]$^{6+}$** to **[Re16ac]$^{16+}$**) were smaller than the values expected from the data for shorter Re(I) oligomers (**[Re2ac]$^{2+}$** to **[Re5ac]$^{5+}$**). The shapes of the longer Re(I) polymers are probably not rodlike in solution, but are more condensed forms, because of aggregation. This will be discussed later.

$$\log M_W = -0.977K_{SEC} + 5.891 \text{ (for } \mathbf{[Re6ac]^{6+}} \text{ to } \mathbf{[Re16ac]^{16+}}) \quad (7)$$

Application of eq 7 shows that the number of Re(I) units of the longest isolated polymer made from **[Re5ac]$^{5+}$** is 20.6 ± 3.7. Although the structure of the long Re(I) polymer with >16 Re(I) units could not be determined by ESI FTMS, the logical conclusion based on the results of ^{1}H NMR, IR, and SEC is that the longest isolated polymer made from **[Re5ac]$^{5+}$** is **[Re20ac]$^{20+}$**.

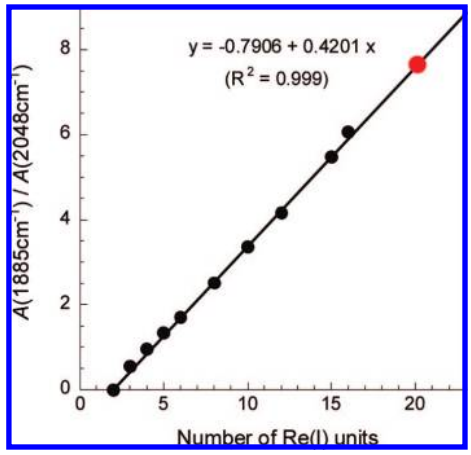

Figure 6. Relationship between the ratios of the ν(CO) peak areas due to edge units (2048 cm^{-1}) and interior units (1885 cm^{-1}) of **[Re2ac]**$^{2+}$ to **[Re16ac]**$^{16+}$ (black dots), and the number of Re(I) units. The red circle is the polymer for the longest isolated polymer made from **[Re5ac]**$^{5+}$.

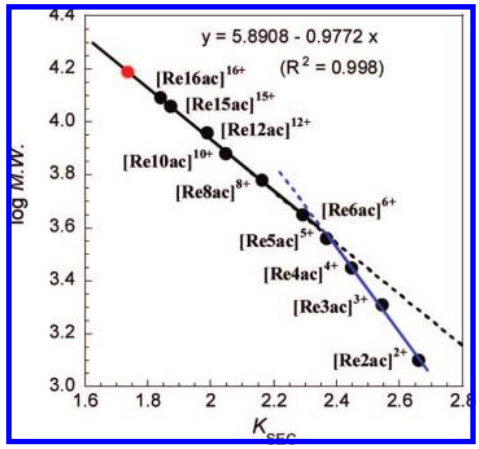

Figure 7. The logarithm of the molecular weight plotted against the distribution coefficient (K_{SEC}) of the Re(I) oligomers and polymers. The red circle shows the longest isolated polymer made from **[Re5ac]**$^{5+}$.

Crystal Structure. X-ray crystallography was performed on the dimer **[Re2ac]**$^{2+}$(PF_6^-)$_2$, two trimers **[Re3ac]**$^{3+}$(PF_6^-)$_3$ and **[Re3et]**$^{3+}$(PF_6^-)$_3$, and a tetramer **[Re4et]**$^{4+}$(PF_6^-)$_4$ (Figure 8a−d). We believe that these are the first crystallographic data for linear-shaped multinuclear Re(I) complexes. As shown in Figure 8a, the dimer **[Re2ac]**$^{2+}$ has a center of inversion between C(26)−C(27) of the bridge ligand ac, and the trimer **[Re3ac]**$^{3+}$ has a mirror plane in the central Re(2) ion (Figure 8b). The packing diagram of **[Re2ac]**$^{2+}$(PF_6^-)$_2$ clearly shows intermolecular $\pi-\pi$ interaction between the bpy ligands which coordinate two adjacent Re units to each other, as shown by the yellow dotted lines in Figure S4 in Supporting Information.

The bpy ligand coordinated to the central Re unit of **[Re3ac]**$^{3+}$ has two sets of intramolecular $\pi-\pi$ interactions, with two phenyl groups on the phosphorus atoms coordinating to the central Re ion, as shown by the blue dotted lines in Figure 8b. Although the end units of **[Re3ac]**$^{3+}$ also show an intramolecular $\pi-\pi$ interaction between the bpy ligand and one phenyl group of the phosphine ligand, there was no intermolecular $\pi-\pi$ interaction with other trimers. The torsional angle between the P(1)−Re(1) and P(2)−Re(2) bonds of **[Re2ac]**$^{2+}$ (180.0°) was also very different from **[Re3ac]**$^{3+}$ (81.1°). Consequently, the intermolecular $\pi-\pi$ interaction in **[Re2ac]**$^{2+}$ is probably the reason why **[Re2ac]**$^{2+}$ has the "trans"-type structure.

Although the other trimer **[Re3et]**$^{3+}$ had a similar crystal structure to **[Re3ac]**$^{3+}$, i.e. the U-shaped form shown in Figure 8c, there was no mirror plane in **[Re3et]**$^{3+}$, and the torsional angle between the Re(1)−P(1) and Re(3)−P(4) bonds in both the edge units was 31.6° (it was 0° for that of **[Re3ac]**$^{3+}$).

The main chain of the tetramer with et bridge ligands **[Re4et]**$^{4+}$ had a circle-like structure (Figure 8d), so that the distance between the two Re (I) ions in both the edges (6.14 Å) was shorter than the other Re−Re distances (>6.7 Å), and the torsional angle between Re(1)−Re(2) and Re(3)−Re(4) was very small (5.6°). This should provide a clue to the nonlinearity in the plots of the logarithm of molecular weight versus K_{SEC} of the Re(I) oligomers in the SEC analysis (Figure 7); if these multinuclear Re(I) complexes have rod-shaped conformation in solution, these plots should lie on a single straight line. The X-ray crystallographic data for the trimers and the tetramer suggest that extended structures are not feasible for the Re(I) oligomers in the absence of intermolecular interaction, and probably also for longer polymers. Since the K_{SEC} values of the longer polymers than the 6mer in SEC were smaller than the values expected from the plots for the shorter oligomers (Figure 7), the polymers must be intramolecularly aggregated, and possibly have helical structures even in solution.

X-ray crystallographic data of some mononuclear rhenium(I) complexes, *fac*-[Re(LL)(CO)$_3$(PR$_3$)]$^+$ and *cis,trans*-[Re(LL)-(CO)$_2$(PR$_3$)$_2$]$^+$, (LL = bpy, 4,4′-dimethyl-bpy) have been reported by Sullivan's group[30] and ours.[27a,31,32a] There is no serious discrepancy in bond distances and angles around Re(I) between the mono- and multinuclear complexes (Table 2).

UV−Vis Absorption Spectra. Figure 9a shows the UV−vis absorption spectra of PF_6 salts of **[Re2ac]**$^{2+}$ − **[Re20ac]**$^{20+}$ in MeCN. The lowest energy and broadband at 350 nm in the spectrum of **[Re2ac]**$^{2+}$ is assigned to metal-to-ligand charge transfer (MLCT) absorption of both Re(I) tricarbonyl complex units, because of the similarity to those of *fac*-[Re(bpy)(CO)$_3$(PR$_3$)]$^+$ type mononuclear complexes; the absorption at 320 nm can be assigned as an intraligand transition of the bpy ligand ($\pi-\pi^*$).[19] For the other complexes, their MLCT absorption bands were broader and were observed at longer wavelength, and their shapes of the MLCT absorption differed. The complexes **[Re3ac]**$^{3+}$ to **[Re20ac]**$^{20+}$ have two types of Re(I) units, namely the two-edge tricarbonyl complex units [Re(bpy)(CO)$_3$(PPh$_2$)-] and the interior biscarbonyl complex unit(s) [-(PPh$_2$)Re(bpy)(CO)$_2$(PPh$_2$)-]$^+$. Comparison with the corresponding mononuclear complexes, [Re(bpy)-(CO)$_3$(PPh$_3$)]$^+$ and [Re(bpy)(CO)$_2$(PPh$_3$)$_2$]$^+$, shows that the MLCT absorption of the biscarbonyl complex units is red-shifted relative to that of the tricarbonyl complex units.[19,27] This difference should be due to the weaker ligand field strength of the phosphorus ligands than that of the CO ligand. The difference in shape of the MLCT absorption band is therefore understood as due to differences in the number of biscarbonyl complex units in a polymer molecule. Figure 9b shows the subtracted spectra UV−vis absorption spectrum of **[Re2ac]**$^{2+}$

(31) Tsubaki, H.; Tohyama, S.; Koike, K.; Saitoh, H.; Ishitani, O. *Dalton Trans.* **2005**, 385–395.
(32) (a) Tsubaki, H.; Sekine, A.; Ohashi, Y.; Koike, K.; Takeda, H.; Ishitani, O. *J. Am. Chem. Soc.* **2005**, *127*, 15544–15555. (b) Tsubaki, H.; Sugawara, A.; Takeda, H.; Gholamkhass, B.; Koike, K.; Ishitani, O. *Res. Chem. Intermed.* **2007**, *33*, 37–48.

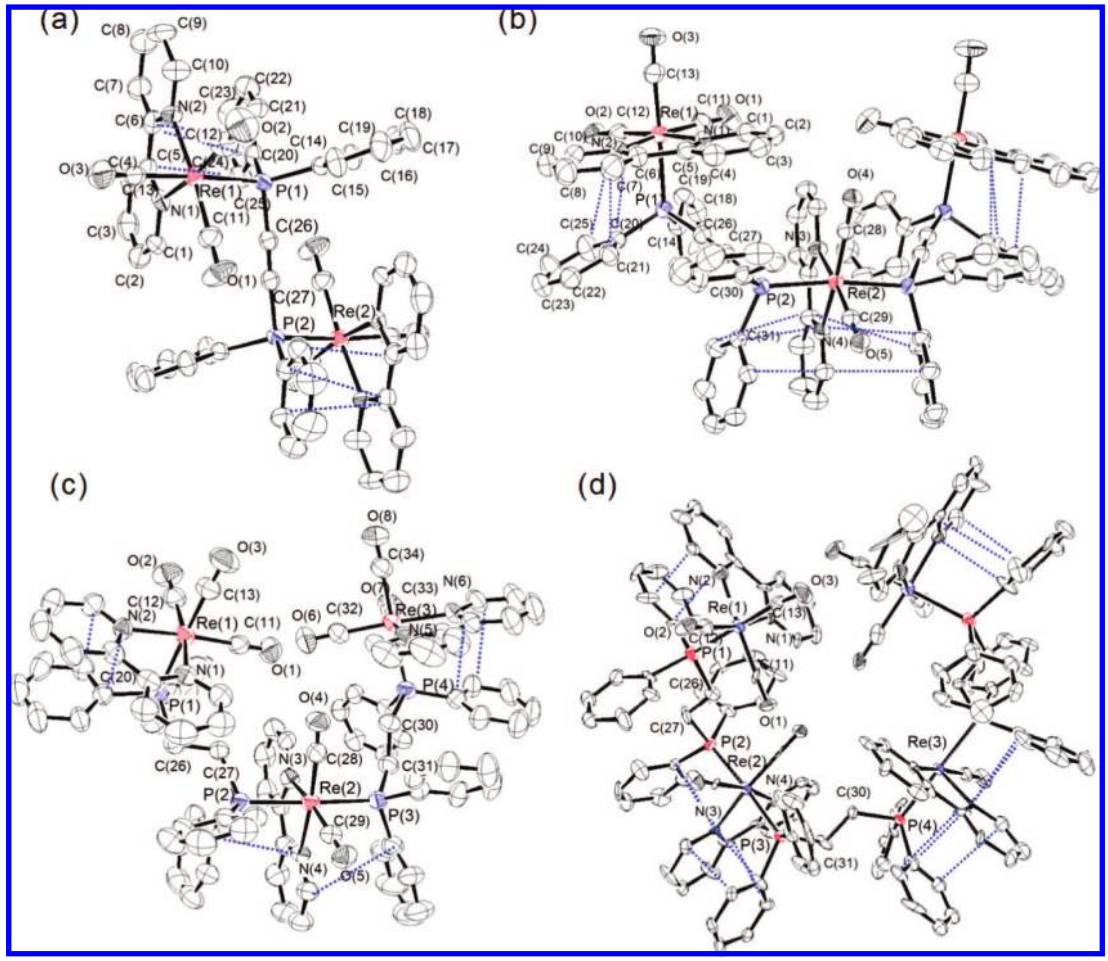

Figure 8. ORTEP drawings of **[Re2ac]**$^{2+}$(PF_6^-)$_2$ (a), **[Re3ac]**$^{3+}$(PF_6^-)$_3$ (b), **[Re3et]**$^{3+}$(PF_6^-)$_3$ (c), and **[Re4et]**$^{4+}$(PF_6^-)$_4$ (d). PF_6^- and hydrogen atoms are omitted for clarity. The ellipsoids correspond to 30% probability.

from these of **[Re3ac]**$^{3+}$ − **[Re20ac]**$^{20+}$, divided by the number of biscarbonyl complex units. The similarity of these spectra indicates that interaction among the complex units is not strong.

The similar subtracted spectra of **[Re2et]**$^{2+}$ from these for **[Re3et]**$^{3+}$ to **[Re7et]**$^{7+}$ which have et as bridge ligand, are shown in Figure 10. The spectrum of mononuclear complex *fac*-[Re(bpy)$(CO)_2(PPh_2Pr)_2$]$^+$ is also shown using a red line in Figure 10, for which the MLCT absorption band was observed at 20 nm longer wavelength. Although the similarity of the subtracted spectra for the oligomers shows that there is no strong interaction among the units in **[Re3et]**$^{3+}$ − **[Re7et]**$^{7+}$, it is possible that the environment around the units in the oligomers differs from that in the mononuclear complex, probably because of the aggregation.

Emission. The multinuclear complexes all emit at room temperature in a degassed MeCN solution upon excitation at 350 nm. Figure 11 shows the emission spectra of **[Re2ac]**$^{2+}$ to **[Re20ac]**$^{20+}$, standardized by the absorbance at the excitation wavelength 350 nm. The emission spectra of **[Re2ac]**$^{2+}$ had a broad band with an emission maximum at 523 nm; the emission showed a single exponential decay with a lifetime of 860 ns. These are typical properties of emission from the ^{3}MLCT excited state of [Re(bpy)$(CO)_3(PR_3)$]$^+$ type complexes.[19,31,33] Emission from the other compounds was observed with an emission maximum at 572 nm. The shape and energy of the emission from all complexes except **[Re2ac]**$^{2+}$ were very similar, although the quantum yields of emission were different; a lower quantum yield was obtained from longer polymers with more Re(I) units. It has been reported that emission from *cis,trans*-[Re(bpy)$(CO)_2(PR_3)_2$]$^+$ type complexes is generally red-shifted by 30−60 nm compared to that from *fac*-[Re(bpy)-$(CO)_3(PR_3)$]$^+$.[19,27,31,32a] Figure 11 therefore indicates that efficient intramolecular energy transfer occurs from the edge units [Re(bpy)$(CO)_3$-] to the interior units [-Re(bpy)$(CO)_2$-].

The emission decay profiles from **[Re3ac]**$^{3+}$ to **[Re20ac]**$^{20+}$ were not single exponential. The decay curves could be fitted with double-exponential functions, with lifetimes of 11 and 833 ns in the case of **[Re3ac]**$^{3+}$, but triple-exponential functions (eq 8) were necessary to fit the decay from **[Re4ac]**$^{4+}$ to **[Re20ac]**$^{20+}$, where $I_{em}(t)$, A_n, and τ_n respectively denote intensities of emission, pre-exponential factors, and lifetimes (Table 3).

$$I_{em}(t) = A_1 e^{-t/\tau_1} + A_2 e^{-t/\tau_2} + A_3 e^{-t/\tau_3} \quad (8)$$

Proportions of the pre-exponential factors of each component strongly depend on both excitation and detection wavelengths. As an example, curves a and b of Figure 12 show the decay curve of **[Re8ac]**$^{8+}$ obtained with excitation wavelength 365 nm. As shown in Figure 12a, a monitoring wavelength of 500 nm, which is close to the emission maximum of the edge Re(I) units, gave a main decay component with lifetime about 10 ns,

(33) Hori, H.; Johnson, F. P. A.; Koike, K.; Takeuchi, K.; Ibusuki, T.; Ishitani, O. *J. Chem. Soc., Dalton Trans.* **1997**, *6*, 1019–1023.

Table 2. Selected Bond Lengths (Å) and Angles (deg) for **[Re2ac]**$^{2+}$$(PF_6^-)_2$, **[Re3ac]**$^{3+}$ $(PF_6^-)_3$, **[Re3et]**$^{3+}$$(PF_6^-)_3$, and **[Re4et]**$^{4+}$$(PF_6^-)_4$

	[Re2ac]$^{2+}$$(PF_6^-)_2$	**[Re4et]**$^{4+}$$(PF_6^-)_4$	
		edge unit	interior unit
Bond Lengths			
Re−P	2.499(11)	2.472(4), 2.490(4)	2.404(3), 2.408(4) 2.405(3), 2.418(3)
Re−N	2.177(5) 2.159(5)	2.133(10), 2.161(9) 2.149(12), 2.177(12)	2.174(10), 2.202(10) 2.106(10), 2.178(9)
Re−C	1.966(5)[a] 1.933(7)[b] 1.934(7)[b]	2.023(15)[a], 1.942(15)[b] 1.906(16)[b], 1.945(15)[a] 1.908(12)[b], 1.898(14)[b]	1.777(19), 1.933(14) 1.917(13), 1.927(13)
C−O	1.087(7)[a] 1.124(9)[b] 1.128(8)[b]	1.127(16)[a], 1.146(16)[b] 1.149(16)[b], 1.149(16)[a] 1.161(14)[b], 1.146(14)[b]	1.119(14), 1.249(19) 1.147(14), 1.141(14)
Re−Re	7.676(2)	6.1204(5)	7.1551(6)[d]
P−P	4.746(3)	4.521(3), 4.499(3), 4.479(5)	
Bond Angles			
P−Re−N	81.72(12) 90.84(13)	87.7(3), 85.2(3) 86.3(3), 90.0(3)	90.0(3), 90.4(3) 90.2(3), 89.2(2)
P−Re−C[b]	87.67(18) 96.60(19)	89.2(4), 94.8(4) 88.3(4), 95.1(4)	88.8(4), 92.8(3) 86.5(4), 92.5(4)
N−Re−N	74.6(2)	74.7(4), 75.4(5)	74.7(3), 73.9(4)
C[b]−Re−C[b]	91.0(3)	89.4(5), 87.0(6)	91.0(5), 94.6(6)
P−Re−C[a]	175.66(18)	178.1(4), 176.0(4)	−
P-ReP	−	−	176.3(10), 179.5(11)
Re[e]−Re[f]−Re[f]	−	83.59(1), 87.28(1)	

	[Re3ac]$^{3+}$$(PF_6^-)_3$		**[Re3et]**$^{3+}$$(PF_6^-)_3$	
	edge unit	interior unit	edge unit	interior unit
Bond Lengths				
Re−P	2.4507(9)	2.3895(9)	2.4927(12), 2.4724(11)	2.4119(13), 2.4378(13)
Re−N	2.166(3) 2.171(3)	2.170(4), 2.185(4)	2.161(4), 2.170(4) 2.186(4), 2.166(4)	2.174(4), 2.179(3)
Re−C	1.950(4)[a] 1.922(4)[b] 1.939(5)[b]	1.910(5), 1.921(4)	1.949(5)[a], 1.912(5)[b] 1.922(5)[b], 1.974(5)[a] 1.915(6)[b], 1.909(6)[b]	1.904(5), 1.911(5)
C−O	1.139(5)[a] 1.145(4)[b] 1.159(5)[b]	1.155(6), 1.152(6)	1.146(6)[a], 1.150(6)[b] 1.149(6)[b], 1.117(5)[a] 1.151(6)[b], 1.153(6)[b]	1.163(5), 1.147(5)
Re−Re	10.0293(3)[c]	−	8.1244(3)[c]	−
P−P	4.7172(12)		4.5490(16), 4.5449(14)	
Bond Angles				
P−Re−N	87.32(8) 91.91(7)	87.82(2), 92.01(2)	88.56(10), 87.05(10) 87.47(10), 88.26(10)	85.91(11), 91.00(11)
P−Re−C[b]	86.12(11) 91.31(13)	87.67(2), 92.56(2)	90.57(15), 90.91(14) 91.00(15), 92.94(16)	86.72(15), 96.37(16)
N−Re−N	74.65(11)	74.50(15)	74.23(16), 75.31(15)	74.78(13)
C[b]−Re−C[b]	91.17(17)	89.95(19)	91.2(2), 90.5(2)	92.7(2)
P−Re−C[a]	176.64(12)	−	179.16(16), 178.22(17)	−
P−Re−P	−	173.07(4)	−	176.45(4)
Re[e]−Re[f]−Re[f]	85.93(1)		69.15(1)	

[a] The axial CO ligand, which is trans relative to the phosphorus ligand. [b] The equatorial CO ligand, which is cis relative to the phosphorus ligand. [c] Distance between the edge units. [d] Distance between interior units. [e] The edge unit. [f] The interior unit.

and minors with 100 and 734 ns. The first component with a lifetime 10 ns, on the other hand, was observed as a rise by changing the detection wavelength to 650 nm, where emission from the interior Re(I) units is mainly observed (inlet in Figure 12b). The other two components were still observed as decays with $\tau = 113$ and 750 ns, respectively (Figure 12b). Only two decay components, with lifetimes 100 and 710 ns, were observed using an excitation wavelength of 400 nm, which is largely absorbed by the interior Re(I) units, and a detection wavelength of 600 nm (Figure S5 in Supporting Information). Similar triple-exponential functions were also necessary to fit the decay data for the et complexes **[Re4et]**$^{4+}$ − **[Re7et]**$^{7+}$, with lifetimes of 3−6 ns, ∼120 ns, and ∼500 ns (Table 4). These results clearly indicate that the shortest component is due to emission from the ^{3}MLCT excited-state of the edge Re(I) units. In Figure 13 the shape of the emission spectra from each of the three observed species has been extracted from the time-resolved emission spectra of **[Re8ac]**$^{8+}$.[34] The fact that the 10 ns component has an emission maximum around 520 nm, which is similar to that from **[Re2ac]**$^{2+}$, supports the identification. If the rate constants of both radiative and nonradiative decay from the ^{3}MLCT excited-state of the edge Re(I) units in **[Re8ac]**$^{8+}$ are same as those from **[Re2ac]**$^{2+}$, them the rate constant of energy transfer from the excited edge Re(I) unit to the interior Re(I) unit (k_{et}) can be calculated as $k_{et} = k - k'$, where k is the observed rate constant of decay from the ^{3}MLCT excited-state of the edge Re(I) units in **[Re8ac]**$^{8+}$ and k' is the sum of the radiation and nonradiative decay constants of **[Re2ac]**$^{2+}$. Table 3 summarizes the energy transfer rates for **[Re3ac]**$^{3+}$−**[Re20ac]**$^{20+}$ with their photophysical properties; faster rate constants were observed

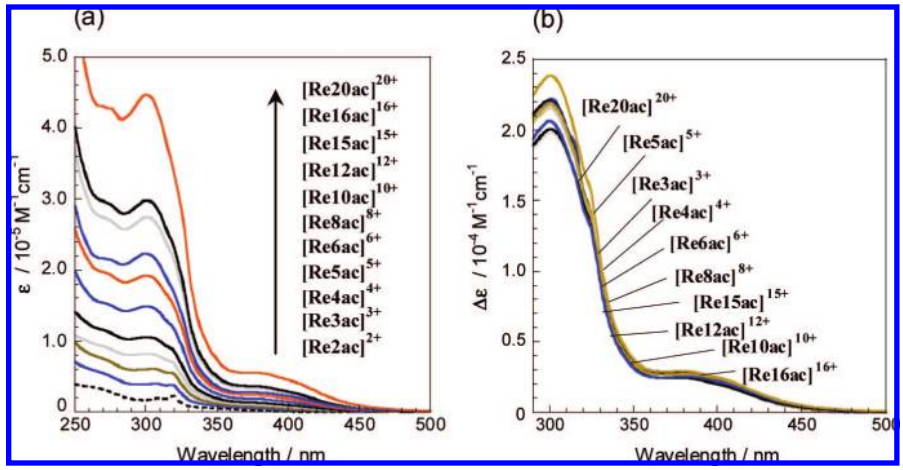

Figure 9. UV−vis absorption spectra of MeCN solutions containing $[Re2ac]^{2+}$ to $[Re20ac]^{20+}$ (a). Subtracted spectra UV−vis absorption spectrum of $[Re2ac]^{2+}$ from those of $[Re3ac]^{3+}$ to $[Re20ac]^{20+}$, divided by the number of biscarbonyl complex units (b).

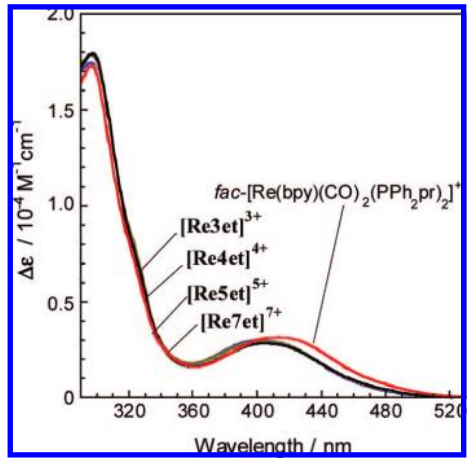

Figure 10. Subtracted spectra UV−vis absorption spectrum of $[Re2et]^{2+}$ from those of $[Re3et]^{3+}$ − $[Re7et]^{7+}$, divided by the number of the biscarbonyl complex units; the red line is the UV−vis absorption spectrum of *fac*-$[Re(bpy)(CO)_2(PPh_2Pr)_2]^+$ in MeCN.

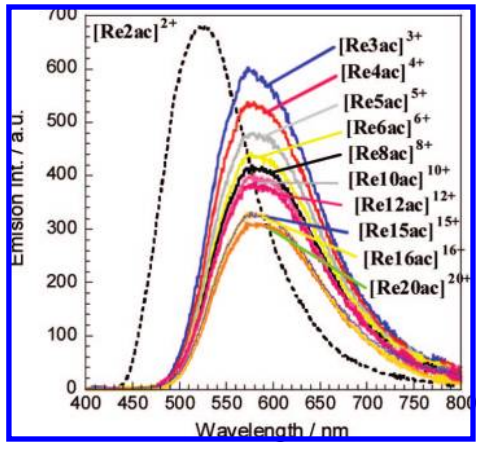

Figure 11. Emission spectra from degassed MeCN solutions containing $[Re2ac]^{2+}$ to $[Re20ac]^{20+}$ standardized by the absorbance at the excitation wavelength 350 nm.

for a longer Re(I) polymer. Similar phenomena were observed in complexes with et as bridge ligands, i.e. $[Re2et]^{2+}$−$[Re7et]^{7+}$ (Table 4). As described in the Isolation and Identification section, the SEC analysis data strongly indicates that the "longer" Re(I) polymers with more than 6 Re(I) units, are aggregated in an MeCN solution. X-ray crystallographic data for $[Re4et]^{4+}$ shows that two edge Re(I) units had a shorter distance even than the distance from the next-door interior unit (Figure 8d). Aggregation in a longer Re(I) polymer therefore probably gives more frequent opportunity for collisions between the excited edge unit and the interior units during the conformation changes in the solution.

The other two components of the emission decay with lifetimes about 100 and 750 ns should be attributed to emission from the interior Re(I) units. This is because, as shown in Figure 13, their emission maxima were respectively 575 and 595 nm and are similar to those from the ^{3}MLCT excited-state of *cis,trans*-$[Re(bpy)(CO)_2(PR_3)_2]^+$ type mononuclear complexes. We have recently reported[32a] that intramolecular $\pi-\pi$ and/or CH$-\pi$ interaction occurs between the diimine ligand and the aryl groups on the phosphorus ligand in $[Re(LL)(CO)_2(PAr_3)_2]^+$ (LL = diimine ligand such as 4,4′-dimethyl-2,2′-bpy); such interligand interaction causes a blue-shift in the emission and longer lifetime of the ^{3}MLCT excited state, which can be explained as follows. The interaction between the ligands gives rise to a smaller polarization in the ^{3}MLCT excited state, because the electron located mainly on the diimine ligand is partially dispersed to the aryl groups. It should reduce the shift between the energy surface minima of the ^{3}MLCT and ground states along the coordination axis. Emission from the ^{3}MLCT to the ground state should then be observed at higher energy, and the Franck−Condon factor becomes smaller, making nonradiative decay slower. We conclude that there are at least two main conformations of $[Re4ac]^{4+}$−$[Re20ac]^{20+}$, respectively; one has interaction between the bpy ligand and the phenyl groups on the ac ligand (λ_{em}^{max} = 575 nm, $\tau \simeq$ 750 ns), but the other has no interaction or much weaker interaction between them (λ_{em}^{max} = 595 nm, $\tau \simeq$ 100 ns). Similar phenomena were observed in for $[Re4et]^{4+}$ - $[Re7et]^{7+}$ ($\tau \simeq$ 120 ns, ∼500 ns: Table 4), and the same explanation applies. This is also supported by the fact that emission of the mononuclear complex *cis,trans*-$[Re(bpy)(CO)_2(PPh_2Pr)_2]^+$ as a model of the interior units in

(34) This was done by normalizing the time resoled emission spectra containing emission from all species. The emission spectrum of the 750 ns component was taken as the time resolved spectrum detected after 1 μs where emission of other species had already decayed. The emission from the 100 ns component was achieved by subtracting the normalized spectrum after 1 μs from the spectrum at 40 ns. Finally the emission spectrum of the 10 ns component was approximated by subtracting the spectrum at 40 ns from the spectrum after 10 ns.

Table 3. Photophysical Properties of **[Re2ac]$^{2+}$** to **[Re20ac]$^{20+}$** in a Deoxygenated Acetonitrile Solution at 25 °C, and Energy Transfer Rates from the Edge Unit to the Interior Unit in **[Re3ac]$^{3+}$** to **[Re20ac]$^{20+}$**

			τ_{em}[d]/ns						
			observed at 480 nm			observed at 575 nm			
complex[a]	λ_{em}[b]/nm	Φ_{em}[c]	τ_1	τ_2	τ_3	τ_1	τ_2	τ_3	$k_{et}/10^7$ s^{-1}
[Re2ac]$^{2+}$	523	0.072	865 (100)	–	–	865 (100)	–	–	–
[Re3ac]$^{3+}$	572	0.073	11 (91)	–	833 (9)	–	–	833 (100)	8.98
[Re4ac]$^{4+}$	572	0.066	11 (73)	128 (7)	798 (20)	–	128 (12)	798 (88)	8.98
[Re5ac]$^{5+}$	571	0.062	11 (83)	112 (1)	796 (16)	–	112 (5)	796 (95)	8.98
[Re6ac]$^{6+}$	571	0.058	11 (57)	129 (5)	768 (38)	–	129 (12)	768 (88)	8.98
[Re8ac]$^{8+}$	572	0.056	10 (86)	110 (2)	763 (12)	–	110 (11)	763 (89)	9.88
[Re10ac]$^{10+}$	572	0.053	8 (81)	168 (12)	720 (8)	–	168 (21)	720 (79)	12.38
[Re12ac]$^{12+}$	572	0.051	7 (82)	118 (4)	758 (14)	–	118 (15)	758 (85)	14.17
[Re15ac]$^{15+}$	572	0.049	4 (96)	162 (4)	–	–	162 (20)	764 (80)	24.88
[Re16ac]$^{16+}$	572	0.048	5 (87)	64 (3)	757 (10)	–	64 (22)	757 (78)	19.88
[Re20ac]$^{20+}$	572	0.046	4 (92)	132 (8)	–	–	132 (14)	747 (86)	24.88

[a] All complexes were PF_6^- salts. The excitation wavelength was 350 nm. [b] Emission maximum. [c] Quantum yield of emission. [d] Lifetime. Numbers in parentheses are percentages of pre-exponential factors, i.e., $A_n/\sum_{m=1}^{3}A_m$ (see eq 8).

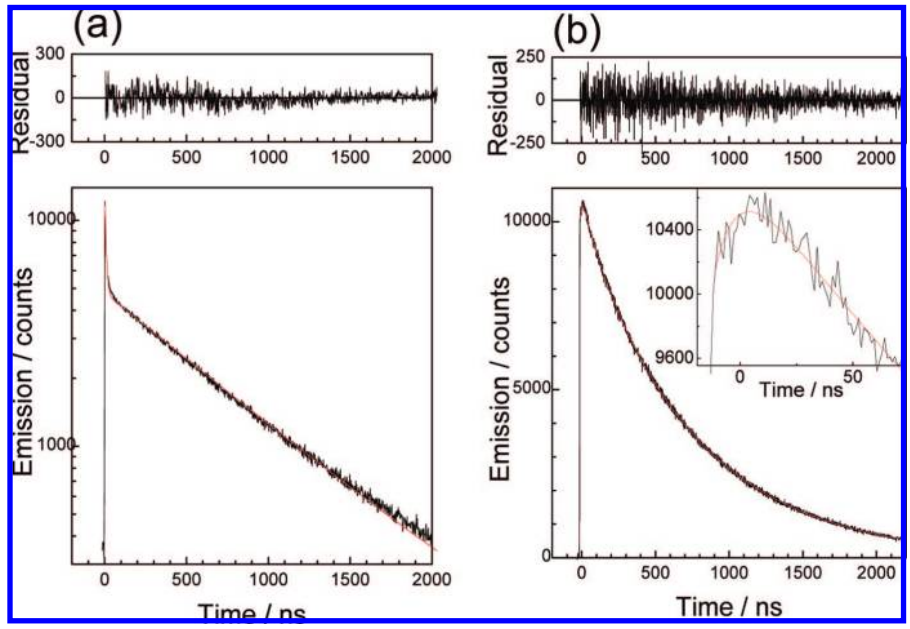

Figure 12. Emission decay curves of **[Re8ac]$^{8+}$** obtained at excitation wavelength of 365 nm. Monitor wavelength: 500 nm (a) and 650 nm (b).

Table 4. Photophysical Properties of **[Re2et]$^{2+}$** to **[Re7et]$^{7+}$** in a Deoxygenated Acetonitrile Solution at 25 °C, and Energy Transfer Rates from the Edge Unit to the Interior Unit in **[Re3et]$^{3+}$** – **[Re7et]$^{7+}$**

			τ_{em}[d]/ns						
			observed at 500 nm			observed at 600 nm			
complex[a]	λ_{em}[b]/nm	Φ_{em}[c]	τ_1	τ_2	τ_3	τ_1	τ_2	τ_3	k_{et} 10^7 s^{-1}
[Re2et]$^{2+}$	543	0.135	865 (100)	–	–	865 (100)	–	–	–
[Re3et]$^{3+}$	626	0.011	6 (83)	143 (17)	–	–	143 (100)	–	1.66
[Re4et]$^{4+}$	628	0.009	4 (99.7)	129 (0.3)	–	–	129 (92)	556 (8)	2.49
[Re5et]$^{5+}$	628	0.008	4 (100)	–	–	–	117 (95)	515 (5)	2.49
[Re7et]$^{7+}$	628	0.007	3 (100)	–	–	–	123 (94)	484 (6)	3.32

[a] All complexes were PF_6^- salts. The excitation wavelength was 350 nm. [b] Emission maximum. [c] Quantum yield of emission. [d] Lifetime. Numbers in parentheses are percentages of pre-exponential factors, i.e., $A_n/\sum_{m=1}^{3}A_m$ (see eq 8).

[Re3et]$^{3+}$ – **[Re7et]$^{7+}$**, exhibits a double exponential decay with lifetimes of 130 and 500 ns. It is noteworthy that some interactions between the bpy ligand and the phenyl groups on **[Re3ac]$^{3+}$**, **[Re3et]$^{3+}$**, and **[Re4et]$^{4+}$** were observed in crystals (Figure 8).

A clear difference in emission behavior between the two series of multinuclear Re(I) complexes with et and ac as bridge ligands is the ratio of the pre-exponential factor obtained for the components with lifetimes 100–130 ns and 500–800 ns. For the ac complexes, the component with longer lifetime was dominant (~90%), but the shorter lifetime component was dominant (>90%) for the et complexes. This suggests that not only the phenyl groups but also the C≡C group on the ac ligand can generate $\pi-\pi$ interaction with the bpy ligand.

The quantum yield of emission decreased in the longer Re(I) polymers in both series, as shown in Figure 11 and Tables 3 and 4. However, there were no significant differences in the emission lifetimes from the interior units, except for the trimer,

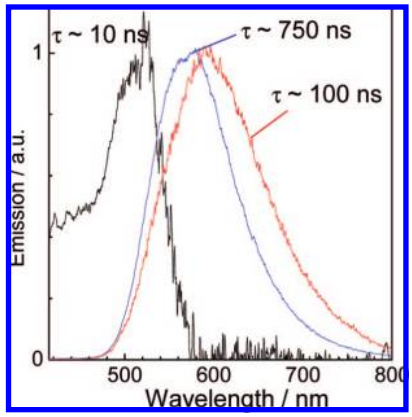

Figure 13. Time resolved emission spectra of **[Re8ac]**$^{8+}$. Black, red, and blue lines are emission spectra with lifetime of 10, 100, and 750 ns, respectively.[34]

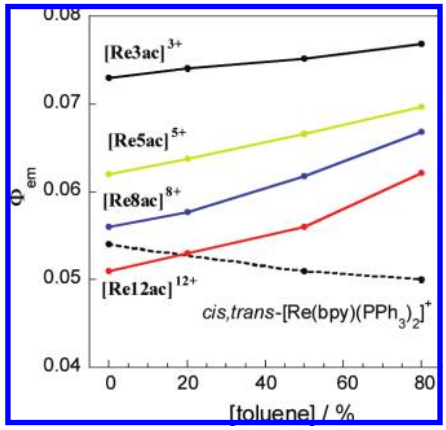

Figure 14. Dependence of Φ_{em} on toluene content in an MeCN/toluene mixed solution.

and the ratios of the pre-exponential factors in any of the polymers. The quantum yields and the lifetimes can be deduced from eqs 9 and 10. The nonradiative decay constant (k_{nr}) should be much larger than the radiative decay constant (k_r), because the quantum yield of emission is less than 10% except for that of **[Re3et]**$^{3+}$ (11%). Consequently, the change of Φ_{em} depending on the number of Re(I) units in the Re(I) polymer should be reflected in differences of k_r, whereas k_{nr} should not change.

$$\Phi_{em} = \frac{k_r}{k_r + k_{nr}} \tag{9}$$

$$\tau = \frac{1}{k_r + k_{nr}} \tag{10}$$

Figure 14 shows the dependence of Φ_{em}, for **[Re3ac]**$^{3+}$, **[Re5ac]**$^{5+}$, **[Re8ac]**$^{8+}$, and **[Re12ac]**$^{12+}$, on the toluene content in MeCN/toluene mixed solutions. In solution containing more toluene, Φ_{em} is greater for the Re(I) polymers. The increase is more pronounced for longer Re(I) polymers. On the other hand, the Φ_{em} value of the mononuclear complex *cis,trans*-$[Re(bpy)(CO)_2(PPh_3)_2]^+$ decreased in solutions containing even more toluene, as shown in Figure 14. Addition of toluene to an MeCN solution probably weakened the hydrophobic (i.e., $\pi-\pi$ and CH$-\pi$) interaction in the Re(I) polymers, and the aggregation of the Re(I) polymers should be partially resolved.[35] In other words, the decrease of k_r for longer Re(I) polymers might be caused by the intramolecular aggregation of the polymer molecules in an MeCN solution.

Conclusion

We applied photochemical ligand substitution reactions of Re(I) diimine complexes with a phosphorus ligand, to find systematic synthetic routes for linear-shaped rhenium(I) oligomers and polymers bridged with bidentate phosphorus ligands. Oligomers and polymers with up to 20 Re(I) units were isolated using SEC and were accurately identified by a combination of ^{1}H NMR, IR, ESI FTMS, analytical SEC, and elemental analysis. All of the synthesized oligomers and polymers were emissive at room temperature in solution. For oligomers and polymers with ≥3 Re(I) units, energy transfer from the edge unit to the interior unit occurs with a rate constant of $(0.9 \times 10^8)-(2.5 \times 10^8)$ s^{-1}. Crystal structures were obtained of some trimers and a tetramer, showing interligand $\pi-\pi$ interaction between the diimine ligand and the phenyl groups on the phosphorus ligand. Both emission and analytical SEC data indicate that the Re(I) polymers aggregate intramolecularly in an MeCN solution. Each unit in the Re(I) oligomers and polymers potentially has photocatalytic activities for CO_2 reduction, and this is currently under investigation in our laboratory.

Experimental Section

Instrumentation and Measurements. IR spectra were recorded in an MeCN solution with a JASCO FT/IR-610 spectrometer at 1-cm^{-1} resolution. ^{1}H and H,H COSY NMR spectra and ^{31}P NMR spectra were measured in an acetone-d_6 solution using a JEOL JNM-AL400 (400 MHz). Residual protons of acetone-d_6 and the phosphorus atom of H_3PO_4 were used as internal and external standards for measurements. Electrospray ionization mass spectroscopy (ESI MS) took place using a Shimadzu LCMS-2010A mass spectrometer or a Thermo Fisher Scientific LTQ Orbitrap ESI FTMS spectrometer. UV−vis absorption spectra were recorded in an MeCN solution with a JASCO V-565 spectrophotometer. Emission spectra were recorded at 25 °C using a JASCO FP-6500 spectrophotometer, with correction for the detector sensitivity determined using correction data supplied by JASCO. The sample solutions were degassed by the freeze−pump−thaw method before the emission measurements. Emission quantum yields were evaluated with $Ru(bpy)_3^{2+}$ ($\Phi_{em} = 0.062$) in degassed acetonitrile as a standard.

Separation and Analysis Using Size Exclusion Chromatography. Separation of the Re oligomer and polymer complexes was achieved by size exclusion chromatography (SEC) using a pair of Shodex PROTEIN KW-2002.5 columns (300 mm × 20.0 mm i.d.) with a KW-LG guard-column (50 mm × 8.0 mm i.d.) and a JAI LC-9201 recycling preparative HPLC apparatus with a JASCO 870-UV detector. The eluent was a 1:1 (v/v) mixture of methanol and acetonitrile with 0.15 M $CH_3CO_2NH_4$, and the flow rate was 5.0 mL min^{-1}. For analysis by SEC, we used a pair of Shodex PROTEIN KW-802.5 (300 mm × 8.0 mm i.d.) with a KW-LG guard-column (50 mm × 6.0 mm i.d.), a JASCO 880-51 degasser, a 880-PU pump, a MD-2010 Plus UV−vis photodiode-array detector and a Rheodyne 7125 injector. The detection wavelength was chosen as 360 nm because all of the complexes analyzed have a strong MLCT and/or $\pi-\pi^*$ absorption bands around 350−500 nm. The column temperature was kept at 40 ± 0.1 °C using a JASCO 860-CO column−oven. The eluent was a 1:1 (v/v) mixture of methanol and acetonitrile with 0.3 M $CH_3CO_2NH_4$, and the flow rate was 0.5 mL min^{-1}. Details have been reported elsewhere.[29]

(35) Addition of methanol (50%) instead of toluene did not cause any change in the emission behavior of the complexes.

Photochemical Reactions. For the photochemical ligand substitution reaction, the solution was irradiated by an Eikosha EHB-WI-500 high-pressure mercury lamp (500 W) with a uranium glass filter (>330 nm) in a Pyrex doughnut-form cell with bubbling of a N_2 or Ar gas. During irradiation, both the reaction vessel and the light source were cooled with tap water.

Crystal Structure Determination. The single crystals of PF_6^- salts of **[Re2ac]**$^{2+}$, **[Re3ac]**$^{3+}$, **[Re3et]**$^{3+}$, and **[Re4et]**$^{4+}$ were obtained by slow diffusion of diethyl ether into an MeCN or an acetone solution containing the complex. Data of **[Re2ac]**$^{2+}$ were collected at 25 °C on an AFC7R, and data of **[Re3ac]**$^{3+}$, **[Re3et]**$^{3+}$, and **[Re4et]**$^{4+}$ were collected at −50 and −150 °C on a Rigaku Mercury CCD with graphite monochromated Mo Kα radiation (λ = 0.7107 Å). The crystal data of these were yellow prisms of approximate dimensions of 0.20 mm × 0.20 mm × 0.20 mm (**[Re2ac]**$^{2+}$), 0.30 mm × 0.10 mm × 0.10 mm (**[Re3ac]**$^{3+}$), 0.15 mm × 0.10 mm × 0.06 mm (**[Re3et]**$^{3+}$), and 0.14 mm × 0.08 mm × 0.03 mm (**[Re4et]**$^{4+}$). For all the crystals, the structures were solved by SHELX-97 programs.[36] Non-hydrogen atoms were refined anisotropically, and hydrogen atoms were generated geometrically.

Emission Lifetime Measurement. An acetonitrile solution of the metal complex was degassed by means of the freeze−pump−thaw method and transferred into a 10 mm × 10 mm × 40 mm quartz cuvette. Emission lifetimes were measured using a Horiba NAES-1100 time-correlated single-photon-counting system. The sample solutions were excited by a NFL-111 ns H_2 lamp with a proper band-pass filter (Toshiba U350). Decay profile simulations were performed by a nonlinear least-squares method.

Measurement of Time-Resolved Emission Spectra. Emission lifetime measurements were made using the second harmonic of Ti:sapphire laser (SpectraPhysics, Tsunami) as an excitation light source. The repetition rate was reduced to 0.1 MHz by an EO modulator (Conoptics). The emission was detected at magic angle configuration using a polarizer and a half-wave-plate. A photomultiplier (Hamamatsu Photonics, R3809U-50) with an amplifier (Hamamatsu Photonics, C5594) and a counting board (PicoQuanta, PicoHarp 300) were used to detect the signal. A monochromator (Oriel, 77250) was placed in front of the photomultiplier to select monitoring wavelength. The system response time was found to be 32 ps fwhm from light scattered from a colloidal solution. The excitation intensity effect on the emission decay was measured using the third harmonic of DCR-3 (Qaunta Ray, fwhm 5 ns). Emission was detected by a photomultiplier (Hamamatsu Photonics, R1563U-01) placed after the monochromator (Oriel 77250). The output of the photomultiplier was connected to a fast oscilloscope (LeCroy, 1.5 GHz 9662C) and sent to PC for further analysis. The response time of the detection system was approximately 700 ps. For the measurement of time-resolved emission spectra, we used a gated-diode array detector with a polychromator (Hamamatsu Photonics, PMA-50, gate time of 5 ns).

Materials. THF was distilled from Na/benzophenone just before use. Acetonitrile was dried three times over P_2O_5 and then distilled from CaH_2 prior to use. Dichloromethane was dried over CaH_2 prior to use. All purified solvents were kept under N_2 before use. Spectral-grade solvents were used for the spectroscopic measurements. Other reagents and solvents were purchased reagent-grade from Kanto Chemical Co., Tokyo Kasei Co., Wako Pure Chemical Industries, and Aldrich Chemical Co. and were used without further purification.

Synthesis. The standard Schlenk techniques were employed for synthesis. *fac*-Re(CO)$_3$(bpy)(CF_3SO_3) was prepared according to the method in the literature.[22b]

cis,trans-[Re(bpy)(CO)$_2$(η^1-ac)$_2$](CF_3SO_3). A tetrahydrofuran solution (100 mL) of *fac*-Re(CO)$_3$(bpy)(CF_3SO_3) (100 mg, 0.17 mmol) with 5 equiv of bis(diphenylphosphino)acetylene (ac) (350 mg, 0.87 mmol) were stirred for 1 day at room temperature in dim light, giving *fac*-[Re(CO)$_3$(bpy)(η^1-ac)](CF_3SO_3), quantitatively. The solution was irradiated using a high-pressure mercury lamp with a uranium glass filter for 12 h, and the solvent was then evaporated under reduced pressure. The residual red solid was washed several times with degassed ether. Yield: 82%. ESI MS in MeCN (*m*/*z*): 1187, [M]$^+$. IR (MeCN): ν_{CO}/cm^{-1} = 1956, 1886.

[Re(bpy)(CO)$_3$(ac)Re(bpy)(CO)$_3$](CF_3SO_3)$_2$, **[Re2ac]**$^{2+}$($CF_3SO_3^-$)$_2$. A THF solution (100 mL) of *fac*-Re(CO)$_3$(bpy)(CF_3SO_3) (700 mg, 1.22 mmol) and 0.5 equiv of ac (240 mg, 0.61 mmol) was refluxed for 3 days in dim light. The precipitated light-yellow powder was filtered off, washed with diethylether, and dried in a vacuum. Yield: 95%. Anal. Calcd for $C_{54}H_{36}F_6N_4O_{12}P_2Re_2S_2$: C, 41.97; H, 2.35; N, 3.63. Found: C, 42.21; H, 2.63; N, 3.85. ^{1}H NMR (δ, 400 MHz, CD_3COCD_3): 8.78 (d, 4H, *J* = 5.6 Hz, *bpy*-6,6′), 8.28 (d, 4H, *J* = 8.5 Hz, *bpy*-3,3′), 8.12 (dd, 4H, *J* = 8.5, 7.7 Hz, *bpy*-4,4′), 7.65 (m, 4H, *Ph-p*), 7.54−7.44 (m, 8H, *Ph-m*), 7.46 (dd, 4H, *J* = 7.7, 5.6 Hz, *bpy*-5,5′), 7.25 (m, 8H, *Ph-o*). ^{31}P NMR (δ, 400 MHz, CD_3COCD_3): 3.30 (s). IR (MeCN): ν_{CO}/cm^{-1} = 2049 (s), 1965 (m), 1931 (m). ESI MS in MeCN (*m*/*z*): 623 [M]$^{2+}$.

[Re(bpy)(CO)$_3$(ac)Re(bpy)(CO)$_2$(CF_3SO_3)](CF_3SO_3), **[Re2ac(CF$_3$SO$_3$)$_1$]**$^+$($CF_3SO_3^-$). A solution of $CF_3SO_3^-$ salts of **[Re2ac]**$^{2+}$ (150 mg, 0.10 mmol) in 200 mL of THF was irradiated for 25 min. About half of the THF was removed by evaporation, and then diethylether was added to the concentrated solution. Precipitated red powder was filtered off, washed with diethylether, and then dried in a vacuum. Yield: 97%. ESI MS in MeCN (*m*/*z*): 630 [M − CF_3SO_3 + MeCN]$^{2+}$.

[Re(bpy)(CO)$_3$(ac)Re(bpy)(CO)$_2$(η^1-ac)](CF_3SO_3)$_2$, **[Re2ac(η^1-ac)$_1$]**$^{2+}$($CF_3SO_3^-$)$_2$. A dicholoromethane solution (100 mL) of **[Re2ac(CF$_3$SO$_3$)$_1$]**$^+$($CF_3SO_3^-$) (60 mg, 0.04 mmol) and ac (50 mg, 0.13 mmol) was heated at 40 °C for 1 day in dim light. About half of CH_2Cl_2 was removed by evaporation, and diethylether was then added to the concentrated solution. The precipitated orange powder was filtered off, washed with diethylether, and dried in a vacuum. Yield: 90%. ESI MS in MeCN (*m*/*z*): 807 [M]$^{2+}$.

[{Re(bpy)(CO)$_3$(ac)}$_2$Re(bpy)(CO)$_2$](PF_6)$_3$, **[Re3ac]**$^{3+}$(PF_6^-)$_3$. A solution of **[Re2ac(η^1-ac)$_1$]**$^{2+}$($CF_3SO_3^-$)$_2$ (65 mg, 0.03 mmol) and *fac*-Re(CO)$_3$(bpy)(CF_3SO_3) (23 mg, 0.04 mmol) in 100 mL of THF/acetone (1:1) was stirred at room temperature for 1 day, then at 40 °C for 1 day in dim light. The solution was then evaporated. The residue was separated using SEC. The band that included the product was collected and evaporated under reduced pressure. A methanol solution of residue was added dropwise to a concentrated MeOH solution of NH_4PF_6. The precipitated yellow powder was filtered off, washed with diethylether, and dried in a vacuum. Yield: 79%. Anal. Calcd for $C_{90}H_{64}F_{18}N_6O_8P_7Re_3$: C, 43.68; H, 2.61; N, 3.40. Found: C, 43.80; H, 2.56; N, 3.29. ^{1}H NMR (δ, 400 MHz, CD_3COCD_3): 8.71 (d, 4H, *J* = 5.2 Hz, *bpy*-6,6′ of Re(*bpy*)(CO)$_3$-), 8.22 (d, 4H, *J* = 8.0 Hz, *bpy*-3,3′ of Re(*bpy*)(CO)$_3$-), 8.07 (dd, 4H, *J* = 8.0, 7.6 Hz, *bpy*-4,4′ of Re(*bpy*)(CO)$_3$-), 7.97 (d, 2H, *J* = 5.2 Hz, *bpy*-6,6′ of Re(*bpy*)(CO)$_2$-), 7.78 (d, 2H, *J* = 8.0 Hz, *bpy*-3,3′ of Re(*bpy*)(CO)$_2$-), 7.61−7.59 (m, 8H, Ph-*p*), 7.57 (dd, 2H, *J* = 8.0, 7.2 Hz, *bpy*-4,4′ of Re(*bpy*)(CO)$_2$-), 7.54−7.44 (m, 16H, Ph-*m*, and Ph-*o*), 7.42 (dd, 4H, *J* = 7.6, 5.2 Hz, *bpy*-5,5′ of Re(*bpy*)(CO)$_3$-), 7.30−7.10 (m, 16H, Ph-*m*, Ph-*p*, and Ph-*o*), 6.80 (dd, 2H, *J*= 7.2, 5.2 Hz, *bpy*-5,5′ of Re(*bpy*)(CO)$_2$-). ^{31}P NMR (δ, 400 MHz, CD_3COCD_3): 7.87 (s), 2.64 (s). IR (MeCN): ν_{CO}/cm^{-1} = 2048 (s), 1964 (s), 1956 (m), 1930 (m), 1887 (m). ESI MS in MeCN (*m*/*z*): 680 [M]$^{3+}$, 1092 [M + PF_6]$^{2+}$.

[Re(bpy)(CO)$_3$(ac){Re(bpy)(CO)$_2$(ac)}$_2$Re(bpy)(CO)$_3$](PF_6)$_4$, **[Re4ac]**$^{4+}$(PF_6^-)$_4$. A dichloromethane solution (100 mL) of **[Re2ac(CF$_3$SO$_3$)$_1$]**$^+$($CF_3SO_3^-$) (200 mg, 0.13 mmol) and a 0.5 equiv of ac (26.0 mg, 0.066 mmol) was stirred at room temperature for 1 day, and then at 40 °C for 1 day in dim light. The solution was then evaporated. The residue was separated using SEC. The band including the product was collected and evaporated under reduced pressure. A methanol solution of the residue was added dropwise to a concentrated MeOH solution of NH_4PF_6. The precipitated yellow powder was filtered off, washed with diethyl-

(36) Sheldrick, G. M. *SHELX-97. Programs for Crystal Structure Analysis*; University of Göttingen: Germany, 1997.

ether, and then dried in a vacuum. Yield: 72%. Anal. Calcd for $C_{128}H_{92}F_{24}N_8O_{10}P_{10}Re_4$: C, 45.05; H, 2.72; N, 3.28. Found: C, 44.78; H, 2.79; N, 3.15. ^{1}H NMR (δ, 400 MHz, CD_3COCD_3): 8.70 (d, 4H, J = 5.1 Hz, *bpy*-6,6′ of Re(*bpy*)$(CO)_3$-), 8.21 (d, 4H, J = 8.6 Hz, *bpy*-3,3′ of Re(*bpy*)$(CO)_3$-), 8.05 (dd, 4H, J = 8.6, 7.6 Hz, *bpy*-4,4′ of Re(*bpy*)$(CO)_3$-), 7.88 (d, 4H, J = 5.4 Hz, *bpy*-6,6′ of Re(*bpy*)$(CO)_2$-), 7.70 (d, 4H, J = 8.5 Hz, *bpy*-3,3′ in Re(*bpy*)$(CO)_2$-), 7.59−7.53 (m, 16H, Ph-*p*), 7.51 (dd, 4H, J = 8.5, 8.0 Hz, *bpy*-4,4′ of Re(*bpy*)$(CO)_2$-), 7.45−7.38 (m, 28H, Ph-*m*, and Ph-*o*), 7.36 (dd, 4H, J = 7.6, 5.1 Hz, *bpy*-5,5′ of Re(*bpy*)$(CO)_3$-), 7.30−7.10 (m, 16H, Ph-*p*, and Ph-*o*), 6.77 (dd, 4H, J = 8.0, 5.4 Hz, *bpy*-5,5′ in Re(*bpy*)$(CO)_2$-). ^{31}P NMR (δ, 400 MHz, CD_3COCD_3): 7.51 (s), 2.64 (s). IR (MeCN): ν_{CO}/cm^{-1} = 2048 (s), 1962 (s), 1955 (m), 1930 (m), 1884 (m). ESI MS in MeCN (*m*/*z*): 708 $[M]^{4+}$, 993 $[M + PF_6]^{3+}$.

$[Re(bpy)(CO)_3(ac)\{Re(bpy)(CO)_2(ac)\}_3Re(bpy)(CO)_3](PF_6)_5$, **[Re5ac]**$^{5+}(PF_6^-)_5$ and $[Re(bpy)(CO)_3(ac)\{Re(bpy)(CO)_2(ac)\}_5Re(bpy)(CO)_3](PF_6)_7$, **[Re7ac]**$^{7+}(PF_6^-)_7$. A solution of CF_3SO_3 salts of **[Re3ac]**$^{3+}$ (150 mg, 0.06 mmol) in 200 mL of CH_2Cl_2 was irradiated for 1 h. About half of CH_2Cl_2 was removed by evaporation, and diethylether was added to the concentrated solution. The precipitated red powder was filtered off, washed with diethylether, and then dried in a vacuum. A CH_2Cl_2 solution (100 mL) containing the red powder (60 mg) and **[Re2ac(η^1-ac)$_1$]**$^{2+}(CF_3SO_3^-)_2$ (65 mg, 0.03 mmol) was stirred at room temperature for 1 day, then at 40 °C for 1 day in dim light. The solution was then evaporated. The residue was separated using SEC. The bands that included products were collected and evaporated under reduced pressure. A methanol solution of the residue was added dropwise to a concentrated MeOH solution of NH_4PF_6. The precipitated yellow powders were filtered off, washed with diethylether, and dried in a vacuum. Yield: 32% (**[Re5ac]**$^{5+}$) and 4% (**[Re7ac]**$^{7+}$).

Another Synthetic Method of [Re5ac]$^{5+}$(PF_6^-)$_5$. A similar procedure for **[Re4ac]**$^{4+}(PF_6^-)_4$ was applied to the synthesis of **[Re5ac]**$^{5+}(PF_6^-)_5$, using *cis,trans*-$[Re(bpy)(CO)_2(\eta^1\text{-ac})_2](CF_3SO_3)$ instead of ac. Yield: 68%.

[Re5ac]$^{5+}(PF_6^-)_5$: Anal. Calcd for $C_{166}H_{120}F_{30}N_{10}O_{12}P_{13}Re_5$: C, 45.83; H, 2.78; N, 3.22. Found: C, 45.59; H, 2.77; N, 3.32. ^{1}H NMR (δ, 400 MHz, CD_3COCD_3): 8.71 (d, 4H, J = 5.2 Hz, *bpy*-6,6′ of Re(*bpy*)$(CO)_3$-), 8.22 (d, 4H, J = 8.0 Hz, *bpy*-3,3′ of Re(*bpy*)$(CO)_3$-), 8.07 (dd, 4H, J = 8.0, 7.6 Hz, *bpy*-4,4′ of Re(*bpy*)$(CO)_3$-), 7.89 (d, 4H, J = 5.6 Hz, *bpy*-6,6′ of (ii)Re(*bpy*)$(CO)_2$-), 7.82 (d, 2H, J = 5.2 Hz, *bpy*-6,6′ of (iii)Re(*bpy*)$(CO)_2$-), 7.72 (d, 4H, J = 8.4 Hz, *bpy*-3,3′ of (ii)Re(*bpy*)$(CO)_2$-), 7.63 (d, 2H, J = 8.4 Hz, *bpy*-3,3′ of (iii)Re(*bpy*)$(CO)_2$-), 7.56 (dd, 4H, J = 8.4, 8.0 Hz, *bpy*-4,4′ of (ii)Re(*bpy*)$(CO)_2$-), 7.50 (dd, 2H, J = 8.4, 6.4 Hz, *bpy*-4,4′ of (iii)Re(*bpy*)$(CO)_2$-), 7.61−7.55 (m, 16H, Ph-*p*), 7.45−7.38 (m, 30H, Ph-*m*, and Ph-*o*), 7.36 (dd, 4H, J = 7.6, 5.2 Hz, *bpy*-5,5′ of Re(*bpy*)$(CO)_3$-), 7.30−7.10 (m, 34H, Ph-*p*, and Ph-*o*), 6.77 (dd, 4H, J = 8.0, 5.6 Hz, *bpy*-5,5′ in (ii)Re(*bpy*)$(CO)_2$-), 6.73 (dd, 2H, J = 5.2, 6.4 Hz, *bpy*-5,5′ of (iii)Re(*bpy*)$(CO)_2$-). ^{31}P NMR (δ, 400 MHz, CD_3COCD_3): 7.51 (s), 7.14 (s), 2.56 (s). IR (MeCN): ν_{CO}/cm^{-1} = 2048 (s), 1963 (b), 1957 (s), 1930 (m), 1886 (s). ESI MS in MeCN (*m*/*z*): 725 $[M]^{5+}$, 944 $[M + PF_6]^{4+}$.

$[Re(bpy)(CO)_3(ac)\{Re(bpy)(CO)_2(ac)\}_4Re(bpy)(CO)_3](PF_6)_6$, **[Re6ac]**$^{6+}(PF_6^-)_6$ and $[Re(bpy)(CO)_3(ac)\{Re(bpy)(CO)_2(ac)\}_6Re(bpy)(CO)_3](PF_6)_8$, **[Re8ac]**$^{8+}(PF_6^-)_8$. A similar procedure for **[Re5ac]**$^{5+}(PF_6^-)_5$ and **[Re7ac]**$^{7+}(PF_6^-)_7$ was applied to the synthesis of **[Re6ac]**$^{6+}(PF_6^-)_6$ and **[Re8ac]**$^{8+}(PF_6^-)_8$, using **[Re4ac]**$^{4+}(PF_6^-)_4$ instead of **[Re3ac]**$^{3+}(PF_6^-)_3$ as precursor complex.

[Re6ac]$^{6+}(PF_6^-)_6$: Yield 23% based on **[Re4ac]**$^{4+}(PF_6^-)_4$ used. Anal. Calcd for $C_{204}H_{148}F_{36}N_{12}O_{14}P_{16}Re_6$: C, 46.33; H, 2.82; N, 3.18. Found: C, 46.60; H, 3.10; N, 2.94. ^{1}H NMR (δ, 400 MHz, CD_3COCD_3): 8.71 (d, 4H, J = 5.2 Hz, *bpy*-6,6′ of Re(*bpy*)$(CO)_3$-), 8.22 (d, 4H, J = 8.4 Hz, *bpy*-3,3′ of Re(*bpy*)$(CO)_3$-), 8.07 (dd, 4H, J = 8.4, 7.6 Hz, *bpy*-4,4′ of Re(*bpy*)$(CO)_3$-), 7.89 (d, 4H, J = 5.2 Hz, *bpy*-6,6′ of (ii)Re(*bpy*)$(CO)_2$-), 7.82 (d, 4H, J = 5.2 Hz, *bpy*-6,6′ of (iii)Re(*bpy*)$(CO)_2$-), 7.72 (d, 4H, J = 8.4 Hz, *bpy*-3,3′ of (ii)Re(*bpy*)$(CO)_2$-), 7.63 (d, 4H, J = 8.4 Hz, *bpy*-3,3′ of (iii)Re(*bpy*)$(CO)_2$-), 7.56 (dd, 4H, J = 8.4, 8.0 Hz, *bpy*-4,4′ of (ii)Re(*bpy*)$(CO)_2$-), 7.50 (dd, 4H, J = 8.4, 6.4 Hz, *bpy*-4,4′ of (iii)Re(*bpy*)$(CO)_2$-), 7.61−7.55 (m, 16H, Ph-*p*), 7.45−7.38 (m, 34H, Ph-*m*, and Ph-*o*), 7.36 (dd, 4H, J = 7.6, 5.2 Hz, *bpy*-5,5′ of Re(*bpy*)$(CO)_3$-), 7.30−7.10 (m, 50H, Ph-*p*, and Ph-*o*), 6.77 (dd, 4H, J = 8.0, 5.2 Hz, *bpy*-5,5′ in (ii)Re(*bpy*)$(CO)_2$-), 6.73 (dd, 4H, J = 5.2, 6.4 Hz, *bpy*-5,5′ of (iii)Re(*bpy*)$(CO)_2$-). ^{31}P NMR (δ, 400 MHz, CD_3COCD_3): 7.51 (s), 7.14 (s), 2.56 (s). IR (MeCN): ν_{CO}/cm^{-1} = 2048 (s), 1963 (b), 1957 (s), 1930 (m), 1886 (s). ESI MS in MeCN (*m*/*z*): 736 $[M]^{6+}$, 913 $[M + PF_6]^{5+}$.

[Re8ac]$^{8+}(PF_6^-)_8$: Yield 3% based on **[Re4ac]**$^{4+}(PF_6^-)_4$ used. Calcd for $C_{280}H_{204}F_{48}N_{16}O_{18}P_{22}Re_8$: C, 46.94; H, 2.87; N, 3.13. Found: C, 47.17; H, 3.14; N, 3.33. ^{1}H NMR (δ, 400 MHz, CD_3COCD_3): 8.71 (d, 4H, J = 5.2 Hz, *bpy*-6,6′ of Re(*bpy*)$(CO)_3$-), 8.22 (d, 4H, J = 8.4 Hz, *bpy*-3,3′ of Re(*bpy*)$(CO)_3$-), 8.07 (dd, 4H, J = 8.4, 7.6 Hz, *bpy*-4,4′ of Re(*bpy*)$(CO)_3$-), 7.89 (d, 4H, J = 5.2 Hz, *bpy*-6,6′ of (ii)Re(*bpy*)$(CO)_2$-), 7.82 (d, 8H, J = 5.2 Hz, *bpy*-6,6′ of (iii)Re(*bpy*)$(CO)_2$-), 7.72 (d, 4H, J = 8.4 Hz, *bpy*-3,3′ of (ii)Re(*bpy*)$(CO)_2$-), 7.63 (d, 8H, J = 8.4 Hz, *bpy*-3,3′ of (iii)Re(*bpy*)$(CO)_2$-), 7.56 (dd, 4H, J = 8.4, 8.0 Hz, *bpy*-4,4′ of (ii)Re(*bpy*)$(CO)_2$-), 7.50 (dd, 8H, J = 8.4, 6.4 Hz, *bpy*-4,4′ of (iii)Re(*bpy*)$(CO)_2$-), 7.61−7.55 (m, 16H, Ph-*p*), 7.45−7.38 (m, 70H, Ph-*m*, and Ph-*o*), 7.36 (dd, 4H, J = 7.6, 5.2 Hz, *bpy*-5,5′ of Re(*bpy*)$(CO)_3$-), 7.30−7.10 (m, 54H, Ph-*p*, and Ph-*o*), 6.77 (dd, 4H, J = 8.0, 5.2 Hz, *bpy*-5,5′ in (ii)Re(*bpy*)$(CO)_2$-), 6.73 (dd, 8H, J = 5.2, 6.4 Hz, *bpy*-5,5′ of (iii)Re(*bpy*)$(CO)_2$-). ^{31}P NMR (δ, 400 MHz, CD_3COCD_3): 7.54 (s), 7.14 (s), 2.56 (s). IR (MeCN): ν_{CO}/cm^{-1} = 2048 (m), 1956 (s), 1930 (m), 1885 (s). ESI FTMS in MeCN (*m*/*z*): 750.6069 $[M]^{8+}$, 878.4022 $[M + PF_6]^{7+}$, 1048.9623 $[M + 2(PF_6)]^{6+}$, 1287.7479 $[M + 3(PF_6)]^{5+}$, 1645.9264 $[M + 4(PF_6)]^{4+}$.

$[Re(bpy)(CO)_3(ac)\{Re(bpy)(CO)_2(ac)\}_{10}Re(bpy)(CO)_3](PF_6)_{12}$, **[Re12ac]**$^{12+}(PF_6^-)_{12}$ and $[Re(bpy)(CO)_3(ac)\{Re(bpy)(CO)_2(ac)\}_{14}Re(bpy)(CO)_3](PF_6)_{16}$, **[Re16ac]**$^{16+}(PF_6^-)_{16}$. A solution of PF_6^- salts of **[Re4ac]**$^{4+}$ (100 mg, 0.03 mmol) in 150 mL of MeCN was irradiated for 1 h. About half of the MeCN was removed by evaporation, and diethylether was added to the concentrated solution. The precipitated red powder was filtered off, washed with diethylether, then dried in a vacuum. A THF/acetone (1:1) solution (100 mL) containing 0.5 equiv each of the red powder (50 mg) and ac (50 mg, 0.13 mmol) was stirried at room temperature for 1 day, then at 40 °C for 1 day in dim light. The solvent was concentrated by evaporation, then diethylether was added to the concentrated solution. The precipitated orange powder was filtered off, washed with diethylether, then dried in a vacuum. The resulting orange solid (47 mg) and the remains of the red powder (50 mg) were dissolved in 100 mL of a THF/acetone (1:1) solution and stirred at room temperature for 1 day, then at 40 °C for 1 day in dim light. The solution was then evaporated. PF_6 salts of **[Re12ac]**$^{12+}$ and **[Re16ac]**$^{16+}$ were isolated using a similar method of **[Re8ac]**$^{8+}(PF_6^-)_8$ with 55% recovery of the starting complex **[Re4ac]**$^{4+}(PF_6^-)_4$.

[Re12ac]$^{12+}(PF_6^-)_{12}$: Yield 14% based on **[Re4ac]**$^{4+}(PF_6^-)_4$ used. Anal. Calcd for $C_{432}H_{316}F_{72}N_{24}O_{26}P_{34}Re_{12}$: C, 47.54; H, 2.92; N, 3.08. Found: C, 47.77; H, 3.11; N, 3.04. ^{1}H NMR (δ, 400 MHz, CD_3COCD_3): 8.71 (d, 4H, J = 5.2 Hz, *bpy*-6,6′ of Re(*bpy*)$(CO)_3$-), 8.22 (d, 4H, J = 8.4 Hz, *bpy*-3,3′ of Re(*bpy*)$(CO)_3$-), 8.07 (dd, 4H, J = 8.4, 7.6 Hz, *bpy*-4,4′ of Re(*bpy*)$(CO)_3$-), 7.89 (d, 4H, J = 5.2 Hz, *bpy*-6,6′ of (ii)Re(*bpy*)$(CO)_2$-), 7.82 (d, 16H, J = 5.2 Hz, *bpy*-6,6′ of (iii)Re(*bpy*)$(CO)_2$-), 7.72 (d, 4H, J = 8.4 Hz, *bpy*-3,3′ of (ii)Re(*bpy*)$(CO)_2$-), 7.63 (d, 16H, J = 8.4 Hz, *bpy*-3,3′ of (iii)Re(*bpy*)$(CO)_2$-), 7.56 (dd, 4H, J = 8.4, 8.0 Hz, *bpy*-4,4′ of (ii)Re(*bpy*)$(CO)_2$-), 7.50 (dd, 16H, J = 8.4, 6.4 Hz, *bpy*-4,4′ of (iii)Re(*bpy*)$(CO)_2$-), 7.61−7.55 (m, Ph-*p*), 7.45−7.38 (m, Ph-*m*, and Ph-*o*), 7.36 (dd, 4H, J = 7.6, 5.2 Hz, *bpy*-5,5′ of Re(*bpy*)$(CO)_3$-), 7.30−7.10 (m, Ph-*p*, and Ph-*o*), 6.77 (dd, 4H, J = 8.0, 5.2 Hz, *bpy*-5,5′ in (ii)Re(*bpy*)$(CO)_2$-), 6.73 (dd, 16H, J = 5.2, 6.4 Hz, *bpy*-

5,5′ of (iii)Re(*bpy*)(CO)$_2$-). IR (MeCN): ν_{CO}/cm^{-1} = 2048 (m), 1956 (s), 1930 (m), 1885 (s). ESI FTMS in MeCN (*m*/*z*): 946.5232 [M + 2(PF$_6$)]$^{10+}$, 947.6264 [M − CO + MeCN + 2(PF$_6$)]$^{10+}$, 1067.6893 [M + 3(PF$_6$)]$^{9+}$, 1069.0260 [M − CO + MeCN + 3(PF$_6$)]$^{9+}$, 1219.3965 [M + 4(PF$_6$)]$^{8+}$, 1220.9002 [M − CO + MeCN + 4(PF$_6$)]$^{8+}$, 1414.3048 [M + 5(PF$_6$)]$^{7+}$, 1415.8893 [M − CO + MeCN + 5(PF$_6$)]$^{7+}$.

[Re16ac]$^{16+}$(PF$_6^-$)$_{16}$: Yield 3% based on **[Re4ac]**$^{4+}$(PF$_6^-$)$_4$ used. ^{1}H NMR (δ, 400 MHz, CD_3COCD_3): 8.71 (d, 4H, J = 5.2 Hz, *bpy*-6,6′ of Re(*bpy*)(CO)$_3$-), 8.22 (d, 4H, J = 8.4 Hz, *bpy*-3,3′ of Re(*bpy*)(CO)$_3$-), 8.07 (dd, 4H, J = 8.4, 7.6 Hz, *bpy*-4,4′ of Re(*bpy*)(CO)$_3$-), 7.89 (d, 4H, J = 5.2 Hz, *bpy*-6,6′ of (ii)Re(*bpy*)(CO)$_2$-), 7.82 (d, 24H, J = 5.2 Hz, *bpy*-6,6′ of (iii)Re(*bpy*)(CO)$_2$-), 7.72 (d, 4H, J = 8.4 Hz, *bpy*-3,3′ of (ii)Re(*bpy*)(CO)$_2$-), 7.63 (d, 24H, J = 8.4 Hz, *bpy*-3,3′ of (iii)Re(*bpy*)(CO)$_2$-), 7.56 (dd, 4H, J = 8.4, 8.0 Hz, *bpy*-4,4′ of (ii)Re(*bpy*)(CO)$_2$-), 7.50 (dd, 24H, J = 8.4, 6.4 Hz, *bpy*-4,4′ of (iii)Re(*bpy*)(CO)$_2$-), 7.61−7.55 (m, Ph-*p*), 7.45−7.38 (m, Ph-*m*, and Ph-*o*), 7.36 (dd, 4H, J = 7.6, 5.2 Hz, *bpy*-5,5′ of Re(*bpy*)(CO)$_3$-), 7.30−7.10 (m, Ph-*p*, and Ph-*o*), 6.77 (dd, 4H, J = 8.0, 5.2 Hz, *bpy*-5,5′ in (ii)Re(*bpy*)(CO)$_2$-), 6.73 (dd, 24H, J = 5.2, 6.4 Hz, *bpy*-5,5′ of (iii)Re(*bpy*)(CO)$_2$-). IR (MeCN): ν_{CO}/cm^{-1} = 2048 (m), 1956 (s), 1930 (m), 1885 (s). ESI FTMS in MeCN (*m*/*z*): 1077.1376 [M + 4(PF$_6$)]$^{12+}$, 1078.2237 [M − CO + MeCN + 4(PF$_6$)]$^{12+}$, 1188.2388 [M + 5(PF$_6$)]$^{11+}$, 1189.4244 [M − CO + MeCN + 5(PF$_6$)]$^{11+}$, 1321.6564 [M + 6(PF$_6$)]$^{10+}$, 1322.5600 [M − CO + MeCN + 6(PF$_6$)]$^{10+}$, 1484.5049 [M + 7(PF$_6$)]$^{9+}$, 1485.9523 [M− CO + MeCN + 7(PF$_6$)]$^{9+}$, 1688.3134 [M + 8(PF$_6$)]$^{8+}$, 1689.6658 [M − CO + MeCN + 8(PF$_6$)]$^{8+}$, 1950.0658 [M + 9(PF$_6$)]$^{7+}$, 1951.7845 [M − CO + MeCN + 9(PF$_6$)]$^{7+}$.

[Re(bpy)(CO)$_3$(ac){Re(bpy)(CO)$_2$(ac)}$_n$Re(bpy)(CO)$_3$](PF$_6$)$_{n+2}$ (n = 8, 13, and 18), **[Re10ac]**$^{10+}$(PF$_6^-$)$_{10}$, **[Re15ac]**$^{15+}$(PF$_6^-$)$_{15}$, and **[Re20ac]**$^{20+}$(PF$_6^-$)$_{20}$. A similar procedure for PF$_6$ salts of **[Re12ac]**$^{12+}$ and **[Re16ac]**$^{16+}$ was applied to the synthesis of **[Re10ac]**$^{10+}$(PF$_6^-$)$_{10}$, **[Re15ac]**$^{15+}$(PF$_6^-$)$_{15}$, and **[Re20ac]**$^{20+}$-(PF$_6^-$)$_{20}$, using PF$_6$ salts of **[Re5ac]**$^{5+}$ instead of **[Re4ac]**$^{4+}$(PF$_6^-$)$_4$. 50% of the starting complex **[Re5ac]**$^{5+}$(PF$_6^-$)$_5$ was recovered.

[Re10ac]$^{10+}$(PF$_6^-$)$_{10}$: Yield 16% based on **[Re5ac]**$^{5+}$(PF$_6^-$)$_5$ used. Anal. Calcd for $C_{356}H_{260}F_{60}N_{20}O_{22}P_{28}Re_{10}$: C, 47.30; H, 2.90; N, 3.10. Found: C, 47.52; H, 3.05; N, 3.07. ^{1}H NMR (δ, 400 MHz, CD_3COCD_3): 8.71 (d, 4H, J = 5.2 Hz, *bpy*-6,6′ of Re(*bpy*)(CO)$_3$-), 8.22 (d, 4H, J = 8.4 Hz, *bpy*-3,3′ of Re(*bpy*)(CO)$_3$-), 8.07 (dd, 4H, J = 8.4, 7.6 Hz, *bpy*-4,4′ of Re(*bpy*)(CO)$_3$-), 7.89 (d, 4H, J = 5.2 Hz, *bpy*-6,6′ of (ii)Re(*bpy*)(CO)$_2$-), 7.82 (d, 12H, J = 5.2 Hz, *bpy*-6,6′ of (iii)Re(*bpy*)(CO)$_2$-), 7.72 (d, 4H, J = 8.4 Hz, *bpy*-3,3′ of (ii)Re(*bpy*)(CO)$_2$-), 7.63 (d, 12H, J = 8.4 Hz, *bpy*-3,3′ of (iii)Re(*bpy*)(CO)$_2$-), 7.56 (dd, 4H, J = 8.4, 8.0 Hz, *bpy*-4,4′ of (ii)-Re(*bpy*)(CO)$_2$-), 7.50 (dd, 12H, J = 8.4, 6.4 Hz, *bpy*-4,4′ of (iii)Re(*bpy*)(CO)$_2$-), 7.61−7.55 (m, Ph-*p*), 7.45−7.38 (m, Ph-*m*, and Ph-*o*), 7.36 (dd, 4H, J = 7.6, 5.2 Hz, *bpy*-5,5′ of Re(*bpy*)(CO)$_3$-), 7.30−7.10 (m, Ph-*p*, and Ph-*o*), 6.77 (dd, 4H, J = 8.0, 5.2 Hz, *bpy*-5,5′ in (ii)Re(*bpy*)(CO)$_2$-), 6.73 (dd, 12H, J = 5.2, 6.4 Hz, *bpy*-5,5′ of (iii)Re(*bpy*)(CO)$_2$-). IR (MeCN): ν_{CO}/cm^{-1} = 2048 (m), 1956 (s), 1930 (m), 1885 (s).

[Re15ac]$^{15+}$(PF$_6^-$)$_{15}$: Yield 6% based on **[Re5ac]**$^{5+}$(PF$_6^-$)$_5$ used. Anal. Calcd for $C_{546}H_{400}F_{90}N_{30}O_{32}P_{43}Re_{15}$: C, 47.77; H, 2.94; N, 3.06. Found: C, 47.80; H, 3.24; N, 2.76. ^{1}H NMR (δ, 400 MHz, CD_3COCD_3): 8.71 (d, 4H, J = 5.2 Hz, *bpy*-6,6′ of Re(*bpy*)(CO)$_3$-), 8.22 (d, 4H, J = 8.4 Hz, *bpy*-3,3′ of Re(*bpy*)(CO)$_3$-), 8.07 (dd, 4H, J = 8.4, 7.6 Hz, *bpy*-4,4′ of Re(*bpy*)(CO)$_3$-), 7.89 (d, 4H, J = 5.2 Hz, *bpy*-6,6′ of (ii)Re(*bpy*)(CO)$_2$-), 7.82 (d, 18H, J = 5.2 Hz, *bpy*-6,6′ of (iii)Re(*bpy*)(CO)$_2$-), 7.72 (d, 4H, J = 8.4 Hz, *bpy*-3,3′ of (ii)Re(*bpy*)(CO)$_2$-), 7.63 (d, 18H, J = 8.4 Hz, *bpy*-3,3′ of (iii)Re(*bpy*)(CO)$_2$-), 7.56 (dd, 4H, J = 8.4, 8.0 Hz, *bpy*-4,4′ of (ii)-Re(*bpy*)(CO)$_2$-), 7.50 (dd, 18H, J = 8.4, 6.4 Hz, *bpy*-4,4′ of (iii)Re(*bpy*)(CO)$_2$-), 7.61−7.55 (m, Ph-*p*), 7.45−7.38 (m, Ph-*m*, and Ph-*o*), 7.36 (dd, 4H, J = 7.6, 5.2 Hz, *bpy*-5,5′ of Re(*bpy*)(CO)$_3$-), 7.30−7.10 (m, Ph-*p*, and Ph-*o*), 6.77 (dd, 4H, J = 8.0, 5.2 Hz, *bpy*-5,5′ in (ii)Re(*bpy*)(CO)$_2$-), 6.73 (dd, 18H, J = 5.2, 6.4 Hz, *bpy*-5,5′ of (iii)Re(*bpy*)(CO)$_2$-). IR (MeCN): ν_{CO}/cm^{-1} = 2048 (m), 1956 (s), 1930 (m), 1885 (s). ESI FTMS in MeCN (*m*/*z*): 1103.0469 [M + 4(PF$_6$)]$^{11+}$, 1104.1411 [M − CO + MeCN + 4(PF$_6$)]$^{11+}$, 1227.8493 [M + 5(PF$_6$)]$^{10+}$, 1229.0525 [M − CO + MeCN + 5(PF$_6$)]$^{10+}$, 1380.3828 [M + 6(PF$_6$)]$^{9+}$, 1381.8322 [M − CO + MeCN + 6(PF$_6$)]$^{9+}$, 1571.0529 [M + 7(PF$_6$)]$^{8+}$, 1572.8063 [M − CO + MeCN + 7(PF$_6$)]$^{8+}$.

[Re20ac]$^{20+}$(PF$_6^-$)$_{20}$: Yield 4% based on **[Re5ac]**$^{5+}$(PF$_6^-$)$_5$ used. ^{1}H NMR (δ, 400 MHz, CD_3COCD_3): 8.71 (d, 4H, J = 5.2 Hz, *bpy*-6,6′ of Re(*bpy*)(CO)$_3$-), 8.22 (d, 4H, J = 8.4 Hz, *bpy*-3,3′ of Re(*bpy*)(CO)$_3$-), 8.07 (dd, 4H, J = 8.4, 7.6 Hz, *bpy*-4,4′ of Re(*bpy*)(CO)$_3$-), 7.89 (d, 4H, J = 5.2 Hz, *bpy*-6,6′ of (ii)Re(*bpy*)(CO)$_2$-), 7.82 (d, 32H, J = 5.2 Hz, *bpy*-6,6′ of (iii)Re(*bpy*)(CO)$_2$-), 7.72 (d, 4H, J = 8.4 Hz, *bpy*-3,3′ of (ii)Re(*bpy*)(CO)$_2$-), 7.63 (d, 32H, J = 8.4 Hz, *bpy*-3,3′ of (iii)Re(*bpy*)(CO)$_2$-), 7.56 (dd, 4H, J = 8.4, 8.0 Hz, *bpy*-4,4′ of (ii)Re(*bpy*)(CO)$_2$-), 7.50 (dd, 32H, J = 8.4, 6.4 Hz, *bpy*-4,4′ of (iii)Re(*bpy*)(CO)$_2$-), 7.61−7.55 (m, Ph-*p*), 7.45−7.38 (m, Ph-*m*, and Ph-*o*), 7.36 (dd, 4H, J = 7.6, 5.2 Hz, *bpy*-5,5′ of Re(*bpy*)(CO)$_3$-), 7.30−7.10 (m, Ph-*p*, and Ph-*o*), 6.77 (dd, 4H, J = 8.0, 5.2 Hz, *bpy*-5,5′ in (ii)Re(*bpy*)(CO)$_2$-), 6.73 (dd, 32H, J = 5.2, 6.4 Hz, *bpy*-5,5′ of (iii)Re(*bpy*)(CO)$_2$-). IR (MeCN): ν_{CO}/cm^{-1} = 2048 (m), 1956 (s), 1930 (m), 1885 (s).

Acknowledgment. We thank Dr. Shigeru Sakamoto (Thermo Fisher Scientific) for ESI FTMS measurements.

Supporting Information Available: Crystallographic files for the PF$_6^-$ salts of **[Re2ac]**$^{2+}$, **[Re3ac]**$^{3+}$, **[Re3et]**$^{3+}$, and **[Re4et]**$^{4+}$ in CIF format; crystallographic data; ESI MS spectra of **[Re2ac]**$^{2+}$ and **[Re4ac]**$^{4+}$ before and after irradiation; chromatograms of analytical SEC of reaction mixture and isolated **[Re5ac]**$^{5+}$, **[Re10ac]**$^{10+}$, **[Re15ac]**$^{15+}$, and **[Re20ac]**$^{20+}$; packing diagram of **[Re2ac]**$^{2+}$(PF$_6^-$)$_2$; Figure S5, emission decay curve of **[Re8ac]**$^{8+}$. This material is available free of charge via the Internet at http://pubs.acs.org.

JA8044579